Available online at www.sciencedirect.com
ScienceDirect
Geochimica et Cosmochimica Acta 70 (2006) 5403–5425
Geochimica
www.elsevier.com/locate/gca

Noble gases in D'Orbigny, Sahara 99555 and D'Orbigny glass—Evidence for early planetary processing on the angrite parent body

Henner Busemann [*,1], Silvio Lorenzetti [2], Otto Eugster

Physikalisches Institut, University of Bern, Sidlerstr. 5, 3012 Bern, Switzerland

Received 8 August 2005; accepted in revised form 7 August 2006

Abstract

We analyzed the spallogenic, trapped, fissiogenic and radiogenic noble gas components in various bulk samples of the angrites D'Orbigny and Sahara 99555 as well as in glass separates of D'Orbigny. The D'Orbigny glass samples show hints of solar-like noble gases, as deduced from the trapped elemental and Ne isotopic compositions; the bulk samples do not contain detectable amounts of trapped gases. These observations indicate that D'Orbigny experienced a complex history shortly after its formation 4.56 Ga ago. The glass of D'Orbigny most likely represents magma that rose from the interior of the angrite parent body (APB) and was quenched near the surface. Hence, the APB may contain—similar to the interior of Earth and Mars—solar noble gases. This would call into question the suggested trapping mechanism for solar noble gases in the Earth and Mars, which involves the solution of early atmospheres into magma oceans, due to the APB's inability to retain a primordial atmosphere. The first detection of—possibly parentless—radiogenic excess ^{129}Xe and solar noble gases in the glass of D'Orbigny indicates that the interior of APB degassed to a lesser degree than the outer regions. Therefore primordially trapped, fossil ^{129}I was kept. The APB was not completely devolatilized. Sahara 99555 yields a cosmic-ray exposure age of 6.8 ± 0.3 Ma, while D'Orbigny was exposed to cosmic rays for 11.9 ± 1.2 Ma. Both ages are different than those found in the other angrites. Hence, the angrites analyzed so far sampled surface material from the APB that was ejected in at least five events. In contrast to the bulk sample, the D'Orbigny glass separates yield concordant ages of only 3.0 ± 1.1 Ma, apparently suggesting a pre-exposure of the host material. However, such a scenario is unlikely, due to very similar Mn–Cr ages found in the bulk and glass of D'Orbigny. Most likely, this discrepancy is the result of additional, secondary gas-free glass. Such glass might have been formed during the meteorite's entry into the Earth's atmosphere. Isotopically anomalous Xe due to the decay of ^{247}Cm has not been found. The presence of ^{247}Cm in glass of D'Orbigny has been suggested based on Pb isotope constraints.

1. Introduction

Angrites represent a rare group of meteorites that are comprised of 10 approved members. They are basaltic rocks, rich in the refractory elements Ca, Al, Ti and strongly depleted in the alkalis (Mittlefehldt and Lindstrom, 1990; Prinz and Weisberg, 1995; Mittlefehldt et al., 2002). The angrites formed particularly rapidly and early during solar system evolution (Carlson and Lugmair, 2000). It is generally assumed that they are products of igneous crustal processes. The extent and sequence of differentiation, fractional crystallization or partial melting are not clear (Taylor et al., 1993; Mittlefehldt et al., 2002; Floss et al., 2003; Jambon et al., 2005). The angrites D'Orbigny ("D'O"), Sahara 99555 ("S99") and Northwest Africa 1296 ("N12") are vesicular and abundant glass-filled empty spaces occur in the host rock of D'O (McCoy et al., 2002; Mittlefehldt et al., 2002; Varela et al., 2003; Kurat

* Corresponding author. Fax: +202 478 8821.
E-mail address: busemann@dtm.ciw.edu (H. Busemann).
[1] Present address: Department of Terrestrial Magnetism, Carnegie Institution of Washington, 5241 Broad Branch Road NW, Washington, DC 20015-1305, USA.
[2] Present address: Institut für Biomechanik, ETH Zürich, CH-8092 Zürich, Switzerland.

0016-7037/$ - see front matter © 2006 Elsevier Inc. All rights reserved.
doi:10.1016/j.gca.2006.08.015

et al., 2004; Jambon et al., 2005). This provides evidence for magmatism or impact melting on the angrite parent body (''APB''). Results of partial-melting experiments on the CV3 chondrite Allende (Jurewicz et al., 1993, 2004) as well as Rb/Sr systematics (Nyquist et al., 2003) imply that the APB could have CV3 chondrite-like precursors. In contrast, Kurat et al. (2004) and Varela et al. (2003, 2005) postulate that the angrites formed as ''large CAIs'' (Ca- and Al-rich inclusions) from vapor condensation in the solar nebula. They also suggest that D'O glass formed in the nebula. Prinz and Weisberg (1995) favored an origin from a small parent body (few 100 m) enriched in a CAI component, although they did not exclude nebula condensation.

With the exception of Northwest Africa 1670 (''N16'', Mikouchi et al., 2003), angrites experienced neither alteration nor shock metamorphism after their early crystallization (Carlson and Lugmair, 2000; Mittlefehldt et al., 2002). Therefore, most chronometric systems have not been disturbed and have yielded concordant absolute old ages (Table 1). High-precision Pb–Pb ages for Angra dos Reis (''AdoR''), Lewis Cliff 86010 (''L86''), S99 and N12 are in the range ~1–10 Ma after CAI formation and are commonly used as reference points for the formation of the first planetary matter in the solar system. The rapid early crystallization retained several detectable isotope anomalies due to the decay of short-lived, now extinct radionuclides (Table 2). These were used to determine precise relative ages of the angrites (Table 1). However, excess ^{129}Xe due to the decay of ^{129}I with an intermediate half-life of 15.7 Ma has not yet been found (Wasserburg et al., 1977; Hohenberg et al., 1991).

Strontium and O isotope systematics of AdoR and D'O imply the same parent body for all angrites (Greenwood et al., 2003; Tonui et al., 2003; Greenwood et al., 2005). However, AdoR, the eponym of the angrites, may actually sample another APB (Mittlefehldt et al., 2002). Reflectance spectra do not yield an asteroidal analogue for AdoR, whereas D'O and S99 show rough spectral matches with the small asteroids, 289 Nenetta (42 km diameter) and 3819 Robinson (9 km) (Burbine et al., 2001). Recently, it has been suggested that the angrites may originate from Mercury (Papike et al., 2003; Kuehner et al., 2006).

The angrites LEW 87051 (''L87''), Asuka 881371 (''A88''), S99, D'O, N12, N16 are co-magmatic rocks or originate from very similar magmas, while L86 and AdoR crystallized from other source magmas (see Floss et al., 2003, and references therein; Greenwood et al., 2005). This is also evident in the thermal history; AdoR and L86 cooled relatively slowly, whereas the other angrites cooled much more rapidly. This indicates a near-surface origin on the APB. L86 cooled at ~0.35 °C/yr from thick lava at burial depths of 15–170 m of rock or 1–10 m of regolith (McKay et al., 1993). In contrast, the ''quenched'' angrites L87, A88, S99, D'O and N16 cooled at ~10–50 °C/h from thin lava within ~0.5–2 m below the surface (Mikouchi et al., 2000, 2003; Mikouchi and McKay, 2001). Endogenous melting and impact were suggested as heat source for magma formation near the APB surface (Mikouchi et al., 1996). However, no angrite (except for N16) shows shock features (Mittlefehldt et al., 2002; Mikouchi et al., 2003).

Noble gases provide a wide range of additional information on angrites such as cosmic-ray exposure (CRE) ages and hence the number of impact events that transferred the angrites into space (Eugster et al., 2002 and references therein). Gas-retention ages for ^{4}He and ^{40}Ar trace thermal events that may have affected the most volatile noble gases only. ^{244}Pu–Xe ages are determined relative to AdoR, for which a precise absolute Pb–Pb age exists (Table 1). This allows the study of the formation sequence of the angrites, although it is hampered by the uncertain initial abundance of ^{244}Pu (see Section 4.7). Noble gas data for S99 and D'O have only been incompletely published so far (Bischoff et al., 2000; Eugster and Lorenzetti, 2001; Eugster et al., 2002; Garrison and Bogard, 2003; Kurat et al., 2004).

In this paper, we present a comprehensive noble gas study on S99 and D'O. We discuss complete noble gas data sets for bulk samples of both angrites and present data for the noble gas component in glass separates of D'O. Jagoutz et al. (2003) discovered isotopically highly anomalous U in the glass in combination with apparent Pb–Pb ages of 4.7 Ga. This glass would hence be older than the CAIs, which are generally believed to be the first condensates in the solar system. These observations were explained by the decay of ^{247}Cm ($T_{1/2} = 15.6$ Ma). We measured a sample of D'O glass in order to search for fission Xe from the neutron-induced decay of ^{247}Cm in addition to fission Xe from the spontaneous decay of ^{238}U and ^{244}Pu. Additional fission Xe from ^{247}Cm would disturb the ^{244}Pu–Xe chronometer and would lead to too old ages in some angrites (Busemann and Eugster, 2003). Based on distinct noble gas components in D'O bulk and glass, we present the first hints on solar-like noble gases released from the interior of an asteroid and trapped during early volcanism on the angrite parent body.

2. Experimental procedure

We analyzed the noble gases in bulk samples of S99 and D'O and in D'O glass in 2–4 aliquots each in two independent noble gas laboratories. The glass separates have been selected and provided in two batches by M. E. Varela (Varela et al., 2003). A detailed description of the origin of the various glass grains is unavailable. (Note that this was not required for the initial purpose of the glass study.) Our goal was to search for possible isotopically anomalous or excess fission Xe due to the decay of ^{247}Cm (Jagoutz et al., 2003). The gases were totally extracted by pyrolysis at 1700 °C. Gas-free re-extraction steps at 1750 °C show that the samples were completely degassed. Procedures are described by Busemann and Eugster (2002, Laboratory ''108'') and Eugster et al. (1993, Laboratory ''104''). The results are given in Tables 3–5. The uncertainties include

Table 1
Absolute and relative ages of angrites (in Ga)

	Pb–Pb	Al–Mg	Mn–Cr	Sm–Nd	Rb–Sr	Pu–Xe
Angra dos Reis	4555 ± 5[a] 4544 ± 2[b] 4557.80 ± 0.42[c]			4550 ± 40[d] 4564 ± 37[e]	$>4564.2 \pm 0.6$[b,*] ~4558–4562 Ma[f,*]	
LEW 86010	4557.84 ± 0.52[c]		4549.0 ± 1.8[f,*]	4553 ± 34[c] 4530 ± 40[f]	$<4556 \pm 4$ Ma[c,*] ~4558–4562 Ma[f,*]	~4539 ± 40[g,&]
Asuka 881371	4566 ± 24[h] 4567.0 ± 1.8[h]					4533 ± 40[i,&]
Sahara 99555	4566.2 ± 0.1[j]	4561.5 ± 0.7[k,*] <4564.2[l,*] 4562.5 ± 1.2[m,*] 4561.6 ± 0.7[j,*]				4615 ± 15[n,&]
D'Orbigny	4559.0 ± 1.1[o] 4557 ± 2[p] 4555.4 ± 1.9[p] 4556 ± 4[p] 4557 ± 1[p]	4561.5 ± 0.7[k,*] 4562.7 ± 1.1[m,*]	4561.6 ± 0.5[k,#] 4562.9 ± 0.6[p,#]	4600 ± 70[k] 3080 ± 50[r]		4648 ± 17[n,&]
D'Orbigny glass	~4722[s] ~4700[s]		4562.9 ± 0.6[q,#]			4349 ± 46[n,&]
NWA 1296	4566.2 ± 0.1[j]					

[a] Tatsumoto et al. (1973).
[b] Wasserburg et al. (1977).
[c] Lugmair and Galer (1992).
[d] Lugmair and Marti (1977).
[e] Jacobsen and Wasserburg (1984).
[f] Nyquist et al. (1994).
[g] Eugster et al. (1991).
[h] Premo and Tatsumoto (1995).
[i] Weigel et al. (1997).
[j] Baker et al. (2005).
[k] Nyquist et al. (2003).
[l] Bischoff et al. (2000).
[m] Spivak-Birndorf et al. (2005).
[n] This work, apparent, error-weighed age, average method 1 and 2 (Section 4.7).
[o] Jagoutz et al. (2002).
[p] Jagoutz et al. (2003).
[q] Glavin et al. (2004).
[r] Disturbed, Tonui et al. (2003).
[s] Jotter et al. (2003), excess ^{207}Pb due to now extinct ^{247}Cm (Jagoutz et al., 2003).
[*] Relative to Efremovka CAIs (assuming simultaneous formation with Allende CAIs), age 4567.2 ± 0.6 Ma (Amelin et al., 2002).
[#] Relative to Pb–Pb age of LEW 86010 (Lugmair and Galer, 1992).
[&] Relative to Pb–Pb age of AdoR (Lugmair and Galer, 1992).

2σ statistical errors of the analyses. Blank corrections are $\leqslant$12% for He and Ne and in most cases $\leqslant$7% for Ar–Xe. The Xe blank in D'O glass and the Kr blank in D'O bulk amounted to ~40%, while Kr in D'O glass and S99 #4 was corrected for ~15% blank. Results of the decomposition of the noble gases into spallogenic, radiogenic, fissiogenic and trapped components are given in Tables 6 and 7 and described in the following chapter.

3. Results

3.1. Neon

The Ne isotopic composition in all samples is shown in Fig. 1. While the bulk data for S99 and D'O indicate almost pure spallation (sp) Ne composition, produced during the exposure of the meteorites in space, the data points for the D'O glass plot in the region between Ne_{sp} and trapped (tr) Ne. We will first deduce $(^{20}Ne/^{22}Ne)_{tr}$ for D'O glass: The average chemical compositions of both D'O bulk and glass (Tables A1 and A2) are very similar for the major target elements that are responsible for the production of Ne_{sp}. Hence, we extrapolated the data points for Ne in D'O bulk through the error-weighed data point of D'O glass to obtain the $(^{20}Ne/^{22}Ne)_{tr}$ ratio in D'O glass. Assuming $(^{21}Ne/^{22}Ne)_{tr} = 0.0326 \pm 0.0010$ (solar, Wieler, 2002b), this extrapolation leads to $(^{20}Ne/^{22}Ne)_{tr} = 11.9 \pm 0.3$. This ratio is intermediate between solar wind (SW) and fractionated SW, previously known as solar energetic particles composition (SEP; Grimberg et al., 2006). We determined

Table 2
Extinct radionuclides in angrites

	^{26}Al	^{53}Mn	^{182}Hf	^{247}Cm	^{129}I	^{244}Pu	^{146}Sm
Half life (Ma)	0.716	3.7	9	15.6	15.7	80.0	103
Angra dos Reis	✓[a]	✓[b]	✓[c]		n.d.[d–i]	✓[d–i]	✓[g,j]
LEW 86010	n.d.[k]	✓[b,l]			n.d.[i]	✓[i,m]	✓[k,l]
Asuka 881371		✓[n]				✓[o]	
Sahara 99555	n.d.[p] ✓[a,q,r]	✓[q,s]			n.d.[t]	✓[t]	
D'Orbigny	✓[a,q,r]	✓[r,s,u]		✓[v]	✓[t]	✓[t]	✓[q], n.d.[w]
NWA 1296	✓[a]						
NWA 1670		✓[n]				✓[x]	

n.d., not detected.
[a] Baker et al. (2005).
[b] Lugmair and Shukolyokov (1998).
[c] Quitté et al. (2000).
[d] Wasserburg et al. (1977).
[e] Munk (1967).
[f] Hohenberg (1970).
[g] Lugmair and Marti (1977).
[h] Hohenberg et al. (1981).
[i] Hohenberg et al. (1991).
[j] Jacobsen and Wasserburg (1984).
[k] Lugmair and Galer (1992).
[l] Nyquist et al. (1994).
[m] Eugster et al. (1991).
[n] Sugiura et al. (2003).
[o] Weigel et al. (1997).
[p] Bischoff et al. (2000).
[q] Nyquist et al. (2003).
[r] Spivak-Birndorf et al. (2005).
[s] Sugiura (2002).
[t] This work.
[u] Glavin et al. (2004).
[v] Jagoutz et al. (2003).
[w] Tonui et al. (2003).
[x] Miura et al. (2004).

Table 3
He, Ne and Ar in bulk samples of D'Orbigny and Sahara 99555 and in D'Orbigny glass

Sample	Laboratory	Mass (mg)	^{4}He (10^{-8} cm^3/g)	^{4}He/^{3}He	^{20}Ne (10^{-8} cm^3/g)	^{20}Ne/^{22}Ne	^{21}Ne/^{22}Ne	^{40}Ar (10^{-8} cm^3/g)	^{36}Ar/^{38}Ar	^{40}Ar/^{36}Ar
S99 #1	104	21.40	17030 ± 700	1553 ± 20	1.58 ± 0.07	1.05 ± 0.05	0.823 ± 0.012	218 ± 10	1.00 ± 0.03	153 ± 6
S99 #2	104	20.89	15430 ± 600	1455 ± 20	1.34 ± 0.05	0.898 ± 0.016	0.828 ± 0.010	210 ± 10	1.00 ± 0.03	157 ± 6
S99 #3	108	170.31						268 ± 90	0.984 ± 0.010	151.2 ± 2.0
S99 #4	108	62.71						143.5 ± 2.2	0.777 ± 0.024	133.6 ± 2.8
D'O #1	104	23.24	16535 ± 651	871 ± 11	2.60 ± 0.16	0.92 ± 0.06	0.803 ± 0.017	85 ± 3	0.78 ± 0.06	52 ± 3
D'O #2	104	27.04	13371 ± 519	734 ± 8	2.46 ± 0.10	0.840 ± 0.020	0.820 ± 0.009	62 ± 3	0.732 ± 0.009	43.5 ± 1.9
D'O #3	108	378.91						57 ± 3	0.679 ± 0.005	33.5 ± 0.4
D'O Glass #1	108	93.63	1990 ± 191	781 ± 106	7.32 ± 0.23	5.41 ± 0.28	0.4841 ± 0.002	189.9 ± 1.7	1.940 ± 0.026	74.8 ± 0.3
D'O Glass #2	104	20.03	1721 ± 53	387 ± 10	6.39 ± 0.25	5.9 ± 0.5	0.61 ± 0.12	109 ± 5	1.96 ± 0.10	65.8 ± 2.8

the $^{20}Ne_{tr}$ and $^{21}Ne_{cosm}$ concentrations for D'O glass (Table 6) using the trapped composition determined here. For D'O and S99 bulk, $(^{20}Ne/^{22}Ne)_{tr}$ is unconstrained (Fig. 1) and we accordingly use the range between 9.8 (air) and 13.6 (solar, Wieler, 2002b). $(^{21}Ne/^{22}Ne)_{tr}$ ranges from 0.029 (air) to 0.0326 (solar, Wieler, 2002b). In the bulk samples, a small amount of Ne_{tr} is present in S99 #1 (Table 3).

To determine the CRE ages we used production rates obtained from two, chemistry-depending models that describe the production of spallogenic nuclides from the most important target elements. We applied the empirically found expressions for achondrites given by Eugster and Michel ("EM", 1995) and production rates for ^{3}He and ^{21}Ne based on a purely physical model ("LE", Leya et al., 2000). Both concepts consider the dependency of

Table 4
Kr in bulk samples of D'Orbigny and Sahara 99555 and in D'Orbigny glass

Sample	^{84}Kr (10^{-12} cm^3/g)	^{78}Kr	^{80}Kr	^{81}Kr	^{82}Kr	^{83}Kr	^{86}Kr
		^{84}Kr ≡ 100					
S99 #3	479 ± 34	0.867 ± 0.020	4.62 ± 0.10	0.0238 ± 0.0009	20.9 ± 0.4	21.1 ± 0.4	30.6 ± 0.5
S99 #4	76.3 ± 2.1	1.98 ± 0.06	7.34 ± 0.25	0.108 ± 0.013	25.4 ± 0.8	27.0 ± 0.8	30.9 ± 1.4
D'O #3	11.8 ± 2.9	25 ± 3	65 ± 9	1.57 ± 0.21	100 ± 13	121 ± 16	17.4 ± 2.2
D'O Glass #1	66 ± 6	(1.50 ± 0.09)[a]	6.7 ± 0.4	0.02 ± 0.05	24.2 ± 1.0	22.3 ± 0.6	31.9 ± 0.9

[a] Unreasonably high. See Table 7.

Table 5
Xe in bulk samples of D'Orbigny and Sahara 99555 and D'Orbigny glass

	^{132}Xe (10^{-12} cm^3/g)	^{124}Xe	^{126}Xe	^{128}Xe	^{129}Xe	^{130}Xe	^{131}Xe	^{134}Xe	^{136}Xe
		^{132}Xe ≡ 100							
S99 #3	79.1 ± 2.6	0.638 ± 0.018	0.695 ± 0.012	7.02 ± 0.12	90.8 ± 0.9	14.08 ± 0.19	75.0 ± 0.8	45.1 ± 0.5	40.1 ± 0.5
S99 #4	31.4 ± 0.4	0.93 ± 0.04	1.69 ± 0.07	7.33 ± 0.14	82.0 ± 1.1	14.9 ± 0.6	76.7 ± 2.0	55.9 ± 1.0	53.0 ± 0.9
D'O #3[a]	16.9 ± 2.2	3.20 ± 0.27	5.3 ± 0.5	10.0 ± 0.9	47 ± 5	9.9 ± 1.1	56 ± 6	79 ± 7	84 ± 7
D'O Glass #1	4.8 ± 1.8	1.43 ± 0.11	2.01 ± 0.17	8.9 ± 0.6	126 ± 5	13.7 ± 0.8	71 ± 3	58.3 ± 2.2	51.9 ± 1.1

[a] The D'O bulk measurement was disturbed by abundant reactive gases.

production on the shielding depth of a given sample that is best monitored by the $(^{22}Ne/^{21}Ne)_{sp}$ ratio (Table 6). The grains of the D'O glass batches are not characterized by a distinct shielding depth. They originate from more expanded regions in the D'O meteorite than the bulk samples, because of the inhomogeneous distribution of the glass in the matrix (Varela et al., 2003). Therefore, the shielding depth of D'O glass must be considered as a large-scale average.

All $(^{22}Ne/^{21}Ne)_{sp}$ ratios are $\geqslant 1.19$ (Table 6), and thus lie on the upper side of the typical range given for Ne_{sp} (Wieler, 2002a), with the exception of D'O glass #2, which shows a large uncertainty. This suggests a very low shielding depth for D'O and S99 in the meteoroid or APB. A large production of $^{22}Ne_{sp}$ relative to $^{21}Ne_{sp}$ due abundant Na can be excluded, because both angrites are highly depleted in Na (see introduction and Table A1).

We used shielding-dependent production rates for ^{3}He and ^{21}Ne and average rates for the insignificantly shielding-dependent isotopes ^{38}Ar and ^{126}Xe, but also ^{83}Kr (see note of Table 8). The used equations (Eugster and Michel, 1995) are given in Table 8. The model by Leya et al. yields production rates for ^{3}He and ^{21}Ne. According to these systematics, the large $(^{22}Ne/^{21}Ne)_{sp}$ ratio of 1.222 ± 0.007 for D'O bulk (Table 6) indicates a shielding depth of <0.5 cm in a meteoroid of only a 5 cm radius. In view of the mass of D'O of 16.55 kg this is impossible. Nevertheless, for comparison, we determined production rates for ^{3}He and ^{21}Ne for these irradiation parameters. We use the equations from Eugster and Michel for further discussion. For D'O glass, the shielding indicator $(^{22}Ne/^{21}Ne)_{sp} = 1.24 \pm 0.06$ (Table 6) does not unambiguously determine the shielding depth and size of the meteoroid. Within the uncertainty, this ratio allows radii between 5 and 85 cm and little shielding. We averaged the respective production rates and included the possible variation into the uncertainties (Table 8). S99 with $(^{22}Ne/^{21}Ne)_{sp} = 1.195 \pm 0.005$ (Table 6) appears to originate from the outermost regions (shielding depth of <2 cm) of a small meteoroid of 10-15 cm radius. All production rates and CRE ages obtained with both methods are shown in Tables 8 and 9.

3.2. Helium

^{4}He in angrites consists of radiogenic ^{4}He (rad), $^4He_{sp}$ and possibly $^4He_{tr}$, whereas ^{3}He is essentially entirely spallogenic. We determined the exposure time to cosmic rays based on $^3He_{sp}$ (Table 6) with the same two models outlined in Section 3.1. For the determination of the He-retention ages, $^4He_{sp}$ was subtracted from the measured ^{4}He, using ^{3}He and $(^4He/^3He)_{sp} = 6.1 \pm 0.3$ (Wieler, 2002a). The adopted U and Th concentrations are listed in Tables A1 and A2. The assumption that $^4He_{tr}$ is not present is certainly valid for the bulk samples of D'O and S99: using $(^4He/^{20}Ne)_{tr} = 850$ (average of values given for the Sun and solar wind, Wieler, 2002b) and $^{20}Ne_{tr}$ from Table 6 sets an upper limit for $^4He_{tr}$ of less than 2% of the measured ^{4}He. The presence of some $^4He_{tr}$ in D'O glass is probable, because of the detection of abundant solar Ne_{tr} (see above). Therefore, the He-retention "age" for D'O glass (Table 10) is only an upper limit. At maximum, 30% of the ^{4}He is trapped. However, a correction for solar $^4He_{tr}$ via $^{20}Ne_{tr}$ (Table 6) is not useful, because in siliceous material ^{4}He is less retentive than ^{20}Ne, and the losses of $^4He_{rad}$ and $^4He_{tr}$ cannot be distinguished from each other.

3.3. Argon

The $^{36}Ar/^{38}Ar$ ratios in all bulk samples (Table 3) are $\leqslant 1$ and thus close to the spallogenic ratio of ~0.65 that is

Table 6
Radiogenic, spallogenic and trapped He, Ne and Ar in bulk samples of D'Orbigny and Sahara 99555 and in D'Orbigny glass

	$^{4}He_{rad}$ (10^{-8} cm^3/g)	$^{40}Ar_{rad}$ (10^{-8} cm^3/g)	$^{3}He_{(\equiv sp)}$ (10^{-8} cm^3/g)	$^{21}Ne_{sp}$ (10^{-8} cm^3/g)	$(^{22}Ne/^{21}Ne)_{sp}$	$^{38}Ar_{sp}$ (10^{-8} cm^3/g)	$^{20}Ne_{tr}$ (10^{-8} cm^3/g)	$^{36}Ar_{tr}$ (10^{-8} cm^3/g)
S99 #1	17,000 ± 700	52 ± 9[a]	11.0 ± 0.5	1.24 ± 0.08	1.19 ± 0.02	1.32 ± 0.10	0.37 ± 0.20	0.56 ± 0.09
S99 #2	15,400 ± 600	51 ± 8[a]	10.6 ± 0.4	1.24 ± 0.05	1.20 ± 0.02	1.24 ± 0.09	b.d.	0.54 ± 0.09
S99 #3		65 ± 61[a]				1.7 ± 0.6		0.7 ± 0.6
S99 #4		84 ± 16[a]				1.34 ± 0.06		0.20 ± 0.04
Average	16,200 ± 800[b]	63 ± 8	10.77 ± 0.18[b]	1.237 ± 0.001[b]	1.195 ± 0.005[b]	1.39 ± 0.10		0.50 ± 0.10
D'O #1	16,400 ± 700	b.d.[a]	19.0 ± 0.8	2.28 ± 0.22	1.23 ± 0.03	2.05 ± 0.22	b.d.	0.30 ± 0.13
D'O #2	13,300 ± 500	8 ± 4[a]	18.2 ± 0.7	2.40 ± 0.12	1.22 ± 0.02	1.93 ± 0.12	b.d.	0.18 ± 0.10
D'O #3		b.d.[a]				2.49 ± 0.16		b.d.
Average	14,500 ± 1,500[b]		18.6 ± 0.4[b]	2.37 ± 0.05[b]	1.222 ± 0.007	2.15 ± 0.17		0.23 ± 0.06[b]
D'O Glass #1	1970 ± 190[c]	189.9 ± 1.7[d]	2.55 ± 0.25	0.64 ± 0.04	1.25 ± 0.09	0.94 ± 0.04	6.63 ± 0.23	1.93 ± 0.04
D'O Glass #2	1,690 ± 50[c]	109 ± 5[d]	4.45 ± 0.18	0.65 ± 0.15	0.91 ± 0.19	0.64 ± 0.04	5.88 ± 0.25	1.27 ± 0.07
Average	1,710 ± 70[b]	181 ± 26[b]	3.8 ± 0.9[b]	0.637 ± 0.003[b]	1.24 ± 0.06[b]	0.80 ± 0.15[b]	6.3 ± 0.4[b]	1.78 ± 0.28[b]

b.d., below detection limit.
[a] Assumption $Ar_{tr} = Ar_{air}$.
[b] Error-weighed average.
[c] D'O glass might contain solar $^{4}He_{tr}$. The numbers given here are thus upper limits for $^{4}He_{rad}$.
[d] Assumption $^{40}Ar_{tr} = 0$.

Table 7
Radiogenic, spallogenic[a] and trapped Kr and Xe in bulk samples of D'Orbigny and Sahara 99555 and D'Orbigny glass

	$^{136}Xe_{fiss}$ (10^{-12} cm^3/g)	^{238}U–$^{136}Xe_{fiss}$[b] (10^{-12} cm^3/g)	$^{136}Xe_{fiss}/^{136}Xe_{total}$ (10^{-12} cm^3/g) (%)	$(^{132}Xe/^{136}Xe)_{fiss}$ (10^{-12} cm^3/g)	$(^{134}Xe/^{136}Xe)_{fiss}$ (10^{-12} cm^3/g)	$(^{78}Kr)_{sp}$ (10^{-12} cm^3/g)	$(^{83}Kr)_{sp}$ (10^{-12} cm^3/g)	$(^{126}Xe)_{sp}$ (10^{-12} cm^3/g)	$(^{84}Kr)_{tr}$ (10^{-12} cm^3/g)	$(^{132}Xe)_{tr}$ (10^{-12} cm^3/g)
S99 #3	10.9 ± 2.9	0.23 ± 0.07	34	0.93 ± 0.38	0.93 ± 0.33	1.21 ± 0.13	4.6 ± 1.5	0.295 ± 0.025	477 ± 34[c]	69 ± 15[c]
S99 #4	8.4 ± 1.2	0.23 ± 0.07	51	0.48 ± 0.21	0.89 ± 0.18	1.04 ± 0.08	5.1 ± 0.39	0.438 ± 0.019	74.0 ± 2.0	27 ± 7
Average						1.08 ± 0.07[d]	5.01 ± 0.22[d]	0.38 ± 0.07[d]		
D'O #3	12.5 ± 2.1	0.25 ± 0.08	88	0.86 ± 0.13	0.91 ± 0.14	2.9 ± 0.7	13 ± 3	0.88 ± 0.11	6.1 ± 1.5	5.4 ± 2.7
D'O Glass #1	1.4 ± 0.5	0.26 ± 0.07	54	0.73 ± 0.24	1.04 ± 0.20	0.57 ± 0.08	0.9 ± 0.5	0.08 ± 0.03	65 ± 6	3.8 ± 1.8

[a] Average Kr_{sp} spectrum from literature data and this work: 78:80:82:83:84:86 = (0.211 ± 0.013):(0.486 ± 0.014):(0.738 ± 0.014):1:(0.429 ± 0.022):(0.0075 ± 0.0075).
[b] Expected concentrations based on U concentrations from Tables A1 and A2, accumulation time 4.5578 Ga, $^{238}\lambda_{sf} \times {}^{136}Y_{sf} = (4.1 \pm 1.1) \times 10^{-18}$ a^{-1}.
[c] Increased Kr and Xe concentrations due to terrestrial contamination introduced during crushing.
[d] Error-weighed average.

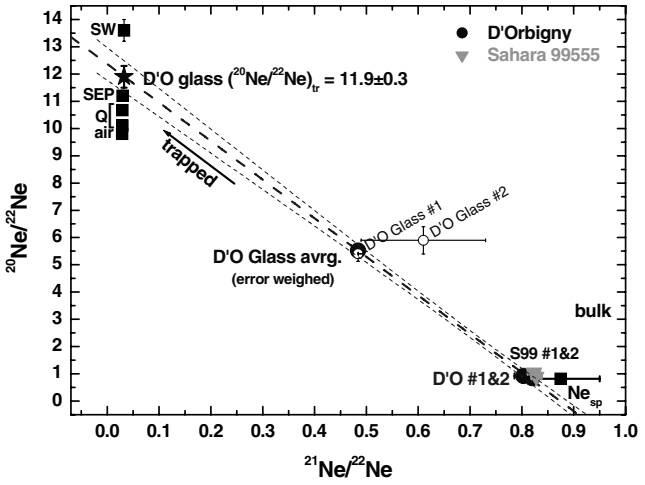

Fig. 1. The Ne isotopic compositions in the bulk samples of D'O and S99 are almost pure spallogenic ("Ne$_{sp}$"; Wieler, 2002a). In contrast, D'O glass is rich in trapped Ne. Extrapolation from Ne$_{sp}$ (≡bulk D'O) through the error-weighed average Ne of D'O glass towards trapped Ne leads to ^{20}Ne/^{22}Ne = 11.9 ± 0.3 (filled star). This is a value typical for samples containing solar noble gases ("SW" and "SEP"; Wieler, 2002b). D'O glass most likely does not contain noble gases from phase Q (Busemann et al., 2000). Confidence limits at the 70% level are shown for comparison.

typically observed in stone meteorites (Wieler, 2002a). This indicates that Ar$_{tr}$ cannot be very abundant (5–40% of the total ^{36}Ar, Table 6). In contrast, D'O glass contains abundant Ar$_{tr}$ (~75% of the total ^{36}Ar, Table 6) and the ^{36}Ar/^{38}Ar ratio is ~1.95 (Table 3). For decomposition we used (^{36}Ar/^{38}Ar)$_{tr}$ = 5.2 ± 0.4, which covers the possibly trapped Ar compositions SW, SEP, air and Q (Busemann et al., 2000; Wieler, 2002b) for D'O glass and (^{36}Ar/^{38}Ar)$_{tr}$ = 5.32 ± 0.05 (air and Q) for the bulk samples. Q noble gases reside in the unknown carbonaceous carrier "phase Q". They are strongly fractionated favoring the heavier isotopes and elements, relative to solar system abundances, and contain most of the heavy, but also some of the light, primordially trapped noble gases in meteorites. We further assumed (^{36}Ar/^{38}Ar)$_{sp}$ = 0.65 ± 0.02. The resulting ^{38}Ar$_{sp}$ and ^{36}Ar$_{tr}$ are given in Table 6, production rates and CRE ages in Tables 8 and 9.

Bulk K–Ar retention ages are difficult to determine since the K content of our samples are not well known. The K concentrations given in the literature are inconsistent and affected by terrestrial contamination to various extents (see Tables A1 and A2). In addition, the correction for atmospheric ^{40}Ar in D'O glass is uncertain. For the bulk samples, we assume that ^{36}Ar$_{tr}$ is completely air. This is justified because neither the isotopic compositions nor the element abundance ratios indicate the presence of solar or Q-gases (see, e.g., Sections 3.1 and 3.4). The calculated K–Ar ages given in Table 10 are based on the "adopted" K concentrations (Tables A1 and A2). In contrast to D'O bulk, the ^{36}Ar$_{tr}$ in D'O glass is not entirely terrestrial, because Ne isotopes and elemental compositions (Sections 3.1 and 3.6) indicate trapped solar noble gases. The element abundance (^{36}Ar/^{132}Xe)$_{tr}$ is 5100 ± 3100 (2σ). This indicates that the trapped component is neither terrestrial contamination (^{36}Ar/^{132}Xe ~ 1300) nor typical meteoritic Q-gas (~75). Finally, the assumption ^{36}Ar$_{tr}$ = ^{36}Ar$_{air}$, used for the bulk samples, would overcorrect the measured ^{40}Ar concentrations by a factor of ~3, because the ^{40}Ar/^{36}Ar$_{tr}$ ratios (Tables 3 and 6) are around 90 and the (^{40}Ar/^{36}Ar)$_{air}$ ratio is 295. As the contributions of ^{40}Ar$_{air}$ to the total ^{40}Ar content are unknown, the ^{40}Ar-retention age of D'O glass is an upper limit.

3.4. Xenon

Xenon (Table 5) in D'O, S99 and D'O glass is a mixture of spallogenic, fission (fiss) and trapped Xe (Fig. 2). Most of the ^{126}Xe is spallogenic, while significant portions of the heavy Xe isotopes are fissiogenic (Table 7). This makes the identification of the trapped Xe component difficult. We decomposed the measured Xe as described by Busemann and Eugster (2002), based on Xe$_{sp}$ spectra given by Hohenberg et al. (1981) and adopted Ba and REE concentrations given in Tables A1–A3. Variations due to the choice of the trapped components Q (Busemann et al., 2000), air and SW (Wieler, 2002b) are included in the uncertainties of ^{126}Xe$_{sp}$ (Table 7) and amount to 0.3%,

Table 8
Production rates deduced from models by Eugster and Michel[a] ("EM", 1995, see also Section 3.1) and Leya et al.[b] ("LE", 2000)

	D'O		D'O glass		S99	
	EM	LE	EM	LE	EM	LE
^{3}He [10^{-10} cm^3/(g Ma)]	159 ± 2	112 ± 3[c]	158 ± 9	130 ± 40	160 ± 3	124 ± 4
^{21}Ne [10^{-10} cm^3/(g Ma)]	15.3 ± 0.7	9.9 ± 0.4[c]	15.3 ± 2.2	14 ± 6	16.8 ± 0.8	12.6 ± 0.8
^{38}Ar [10^{-10} cm^3/(g Ma)]	19.5 ± 1.8		23 ± 5		21.9 ± 1.8	
^{78}Kr [10^{-14} cm^3/(g Ma)]	18.8 ± 1.2		13.6 ± 1.3		16.7 ± 1.8	
^{83}Kr [10^{-14} cm^3/(g Ma)]	111 ± 30		75 ± 23		95 ± 28	
^{126}Xe [10^{-14} cm^3/(g Ma)]	6.9 ± 3.5		4.0 ± 0.5		6.6 ± 1.8	

Chemical compositions taken from Tables A1 and A2. The uncertainties originate from the chemical compositions.

[a] Used equations from EM: (1) and (2) for ^{3}He, (3) and (7) for ^{21}Ne, (10) for ^{38}Ar, and (16) for ^{126}Xe. For ^{83}Kr, we used Eq. (12) for average shielding. This gives CRE ages independent of ^{81}Kr, which is not detectable in D'O glass. Variations due to shielding are in the order of ~20% (Eugster, 1988), which we included systematically in the uncertainty of the production rates.

[b] Shielding and meteoroid sizes as deduced from (^{22}Ne/^{21}Ne)$_{cosm}$ are discussed in Section 3.1.

[c] Determined for (^{22}Ne/^{21}Ne)$_{sp}$ = 1.213, the largest value given in LE (Sections 3.1 and 4.3).

Table 9
Cosmic-ray exposure ages of angrites (Ma)

	This work[a]	Literature	^{3}He[b]	^{21}Ne[b]	^{38}Ar	^{78}Kr	^{81}Kr	^{83}Kr	^{126}Xe
AdoR		55.5 ± 1.2[c]							
L86		17.6 ± 1.0[d]							
L87		$\geqslant 0.2$[d]							
A88		5.4 ± 0.7[e]							
S99	6.8 ± 0.3	6.1 ± 0.2[f]	6.75 ± 0.16 8.7 ± 0.3	7.4 ± 0.3 9.8 ± 0.6	6.4 ± 0.7	6.5 ± 0.8	7.4 ± 1.2	5.3 ± 1.6	5.9 ± 2.0
D'O	11.9 ± 1.2	11.0 ± 0.8[g]	11.71 ± 0.28 (16.6 ± 0.6)[h]	15.5 ± 0.8 (23.9 ± 1.0)[h]	11.1 ± 1.3	15 ± 4	10.7 ± 0.6	12 ± 4	12.9 ± 1.8
D'O glass	3.0 ± 1.1		2.4 ± 0.6 2.9 ± 1.0	(4 ± 8) 4.2 ± 0.6	3.6 ± 1.0	4.2 ± 0.7	n.d.	1.2 ± 0.8	2.1 ± 0.8
NWA 1670		14.7-17.6[i]							

[a] Error-weighed average of all values obtained with the "EM" model (see Section 3.1).
[b] First number: EM model, second number: LE (see Section 3.1).
[c] Lugmair and Marti (1977).
[d] Eugster et al. (1991).
[e] Weigel et al. (1997).
[f] Bischoff et al. (2000), mean of 2 aliquots.
[g] Kurat et al. (2004).
[h] Calculated for $(^{22}Ne/^{21}Ne)_{sp} = 1.213$, the largest value given in LE (Sections 3.1 and 4.3).
[i] Miura et al. (2004).

Table 10
Gas-retention ages of angrites (Ga)

	U/Th–He	Literature	K–Ar	Literature
AdoR		5.0[a] 4.5[b]		<1.93[a] 2.4[b] 4.25[b,c]
L86		3.7 ± 0.7[b]		0.75[b] Disturbed[d]
L87		0.004 ± 0.001[b,e]		
A88		3.75 ± 1.0[f]		3.91 ± 0.5[f]
S99	4.6 ± 0.6[i]	4.1 ± 0.6[g]	1.93 ± 0.19[i]	1.8 ± 0.2[g,h]
D'O	4.2 ± 0.6[i]		1.4 ± 0.7[i]	Disturbed[d]
D'O glass	<0.96[i,j]		3.7 ± 0.7[i]	

[a] Müller and Zähringer (1969).
[b] Eugster et al. (1991).
[c] Recalculated from Müller and Zähringer (1969) adopting a lower K concentration (Eugster et al., 1991).
[d] Terrestrial weathering, Garrison and Bogard (2003).
[e] Most likely almost completely degassed due to solar heating (Eugster et al., 1991).
[f] Weigel et al. (1997).
[g] Bischoff et al. (2000).
[h] Probably too low due to terrestrial contamination.
[i] This work.
[j] Upper limit due to possible solar ^{4}He contributions (Section 3.2).

1.2% and 8% of the average $^{126}Xe_{sp}$ for D'O, D'O glass and S99, respectively. The CRE ages are given in Table 9.

We analysed the heavy noble gases in two bulk samples of S99. The much higher gas concentrations in S99 #3 can be explained by terrestrial contamination that was introduced during crushing of the sample to <750 μm grain size. S99 #4 and D'O remained mostly uncrushed. Kr and Xe concentrations in the crushed sample S99 #3 are larger by a factor of 6.3 and 2.5, respectively, relative to those in S99 #4. The admixture of terrestrial Xe in S99 #3 is also discernable in its Xe isotopic composition that is closer to air Xe than that of S99 #4 (Figs. 2–4).

After subtraction of Xe_{sp} (Table A4), the data for S99, D'O and D'O glass plot between trapped and fission Xe compositions. We applied the same decomposition procedures to all available data sets to assure comparability (Tables A3 and A4). The angrites discussed in the literature as well as the newly measured D'O bulk sample roughly plot on a mixing line between trapped and ^{244}Pu–Xe_{fiss}, indicating that Xe_{fiss} from the decay of ^{238}U is not dominant (Fig. 3). However, the data do not show a clear cut Xe_{tr} composition (Fig. 3) and hence we subtracted (normalised to ^{130}Xe, which is not produced by fission) the average of Q, SW and air–Xe to obtain pure Xe_{fiss} (Table 7). D'O

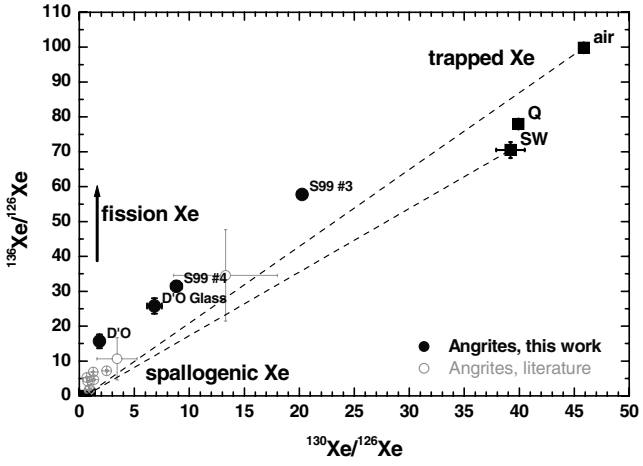

Fig. 2. The Xe isotopic compositions of angrites (bulk samples and separates) plot between trapped and spallogenic Xe. Most data points are shifted to heavier isotopic composition (higher $^{136}Xe/^{126}Xe$ ratios) indicating the presence of fission Xe. The composition of the—usually small—trapped Xe component is not distinguishable. (References: Munk, 1967; Hohenberg, 1970; Lugmair and Marti, 1977; Eugster et al., 1991; Hohenberg et al., 1991; Weigel et al., 1997; for trapped components see Fig. 1).

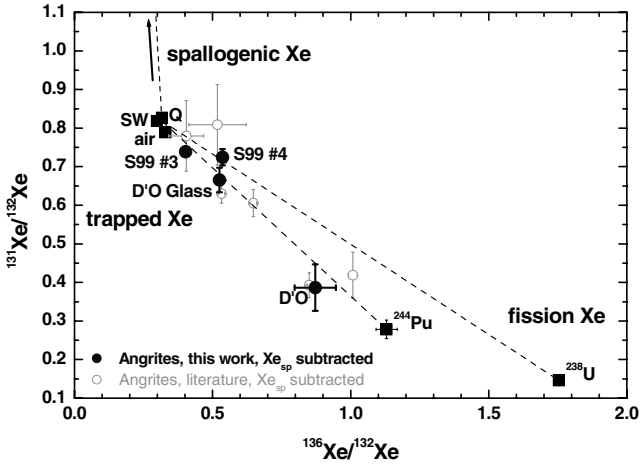

Fig. 3. The compositions of the heavy Xe isotopes in most bulk angrites prove the presence of once live ^{244}Pu. D'O bulk shows a much higher Xe_{fiss}/Xe_{tr} ratio than D'O glass. (References: Munk, 1967; Hohenberg, 1970; Eugster et al., 1991; Hohenberg et al., 1991; Weigel et al., 1997; for trapped components see Fig. 1).

glass may also contain other Xe_{fiss} components, which will be discussed in Section 4.9. The $^{136}Xe_{fiss}$ concentrations and isotopic compositions are listed in Table 7. Contributions from ^{238}U are calculated based on the U concentrations (Tables A1–A3) and a closure time for ^{136}Xe of 4.5578 Ga (Table 1). Xenon contributions from ^{238}U amount to 3–5% in bulk S99 and D'O, but to 32% in D'O glass (Table 7).

Fig. 4 shows the $^{129}Xe/^{132}Xe$ and $^{136}Xe/^{132}Xe$ ratios in all angrites, corrected for Xe_{sp}. The data point for D'O glass indicates an excess of ^{129}Xe (Table 7) due to the decay of short-lived ^{129}I. The data points for all other samples lie

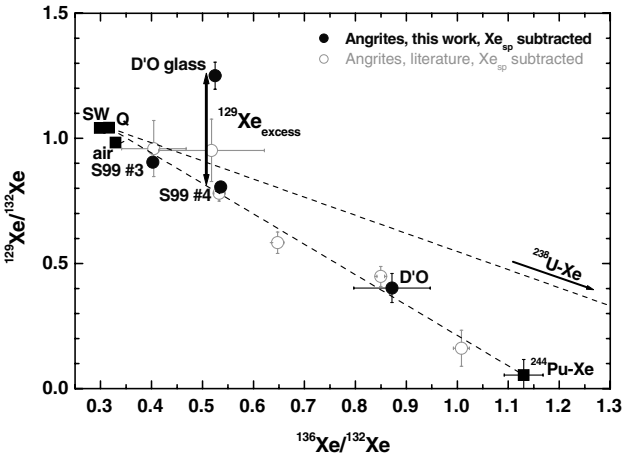

Fig. 4. The Xe isotopic composition of D'O glass shows an excess in ^{129}Xe due to the decay of once live ^{129}I, while D'O bulk and all other bulk angrites plot on the Xe_{tr}–^{244}Pu–Xe mixing line. This is the first report of live ^{129}I in angrites. (References: Munk, 1967; Hohenberg, 1970; Eugster et al., 1991; Hohenberg et al., 1991; Weigel et al., 1997; for trapped components see Fig. 1).

on the mixing lines between trapped and fission Xe. Hohenberg et al. (1991) gave an upper limit of 1×10^{-12} cm^3/g for the ^{129}Xe excess in AdoR and L86. We calculated an excess ^{129}Xe of $(2.2\pm0.4)\times10^{-12}$ cm^3/g for D'O glass. This excess is not the result of a fission reaction for the following reason: the abundance of $^{129}Xe_{fiss}$ relative to $^{136}Xe_{fiss}$ (Table 7) due to the decay of ^{244}Pu and ^{238}U is at maximum 4.8% and 1.5%, respectively (MacNamara and Thode, 1950; Lewis, 1975) and this would lead to a maximum of 0.1×10^{-12} cm^3/g fissiogenic ^{129}Xe. Note that relative $^{129}Xe_{fiss}$ yields from the decay of ^{242}Cm and ^{252}Cf are between 10–20% (Hyde et al., 1964), which might indicate that the yield for ^{238}U is underestimated. However, difficulties in precisely *predicting* fission yields (see discussion of Fig. 9), and the more recent determinations by Hebeda et al. (1987) and Eikenberg et al. (1993), support the use of the value of 1.5%.

3.5. Krypton

Krypton (Table 4) in all samples is a mixture of abundant Kr_{sp}, Kr_{tr} and possibly $^{86}Kr_{fiss}$. We estimated $^{86}Kr_{fiss}$ using Xe_{fiss} from ^{244}Pu and ^{238}U (Table 7) and the $(^{86}Kr/^{136}Xe)_{fiss}$ element ratios given by Wetherill (1953) and Hebeda et al. (1987) for ^{238}U, and Lewis (1975) for ^{244}Pu. Less than 1% of the ^{86}Kr in S99 and D'O glass originate from fission of ^{238}U and ^{244}Pu. In D'O bulk ~14% of the measured ^{86}Kr is fissiogenic (Table 7).

Small excesses of ^{80}Kr (Fig. 5) and ^{82}Kr by neutron-induced reactions ("n") on Br are visible in D'O glass. The $(^{80}Kr/^{82}Kr)_n$ ratio for D'O glass is $\sim0.7\pm0.3$. This value is smaller than those given for thermal and epithermal neutrons (Marti et al., 1966). The $^{80,82}Kr_n$ excesses in the bulk of D'O are too small to be conclusive. N-induced

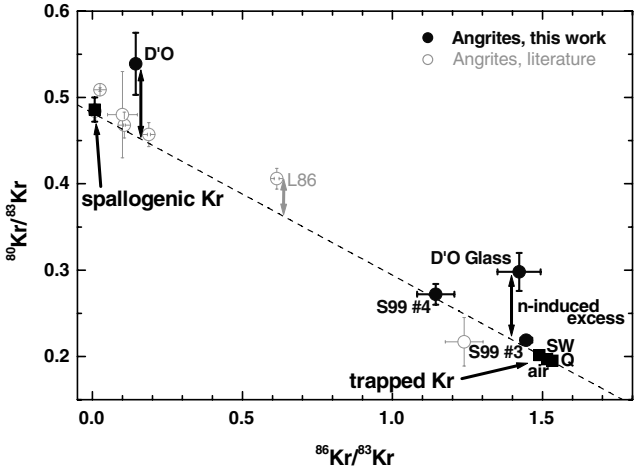

Fig. 5. Glass from the D'O and L86 bulk (Eugster et al., 1991) show small excesses of ^{80}Kr and ^{82}Kr due to the capture of thermal to epithermal neutrons on Br. Secondary neutrons can be observed only in large meteoroids or the uppermost layers of an atmosphere-less parent body. The presence of ^{129}I in the glass may imply that the small excesses are due to an overabundance of Br in the glass relative to the bulk.

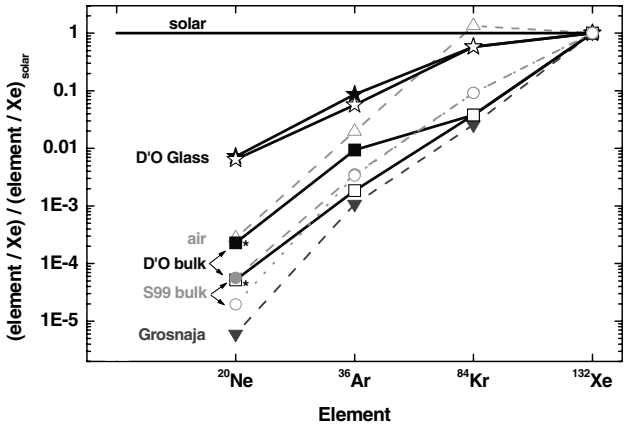

Fig. 6. The trapped noble gases in S99, D'O bulk and D'O glass normalised to ^{132}Xe and solar composition (Wieler, 2002b). The elemental composition of the noble gases in D'O glass indicates a solar origin, while the trapped noble gases in D'O bulk are 'meteoritic", i.e., much more severely fractionated relative to solar gases, and thus similar to those in S99, other achondrites (Busemann and Eugster, 2002) or, e.g., the carbonaceous chondrite Grosnaja (Busemann et al., 2000). The He/Xe, Ne/Xe and Ar/Xe data for D'O glass are calculated with the one available ^{132}Xe abundance (D'O #3). The S99 data are calculated with the ^{132}Xe abundance from S99 #4, which is less affected by air contamination. The Ne/Xe ratios in D'O bulk and S99 #2 (*) are upper limits; the uncertainties of the trapped Ne concentrations allow also for a complete lack of trapped Ne (Table 6).

^{80,82}Kr excess was previously found only in L86 (Eugster et al., 1991).

The decomposition into Kr_{sp} and Kr_{tr} (Table 7) is described by Busemann and Eugster (2002): The trapped components Q, air and SW are considered to determine $^{83}Kr_{sp}$, and the uncertainty of $^{83}Kr_{sp}$ includes these possibilities. The averaged Kr_{sp} isotopic composition for angrites based on data from this work and literature data (Munk, 1967; Eugster et al., 1991; Weigel et al., 1997) is given in a footnote of Table 7. The CRE ages obtained from spallogenic ^{78}Kr and ^{83}Kr (Table 9) are determined with the production rates from EM. The ^{81}Kr/Kr CRE age for S99 is calculated according to the systematics as cited by Eugster (1988, Eq. (3)), however, with an isobaric fractional yield of ^{81}Kr of 0.92 instead of 0.95 (see Eugster, 2003, Eq. (6)). Finally, the ^{81}Kr/Kr CRE age for D'O is deduced with Eq. 4 from Eugster (1988), because of the neutron produced excess in ^{80}Kr and ^{82}Kr (Fig. 5) in D'O. We used a half-life of ^{81}Kr of 0.229 Ma (see Eugster, 2003). The comparison of S99 #3 with S99 #4 shows the significant influence of crushing on the concentration of trapped heavy noble gases (Table 7).

3.6. Elemental composition

The elemental compositions of the trapped noble gases (Tables 6 and 7) in S99, D'O and D'O glass, normalised to $^{132}Xe_{tr}$ and solar composition (Wieler, 2002b), are shown in Fig. 6. The trapped noble gases in D'O glass are much closer to solar composition than the noble gases in the bulk samples of D'O or S99. The observation of a solar-like elemental composition corresponds with the solar Ne_{tr} isotopic composition (Fig. 1). Note that ^{20}Ne, ^{36}Ar and ^{84}Kr in D'O glass are also largely enriched by factors of >2000, ~1.5 and ~3, respectively, relative to the noble gases in the E chondrite South Oman, if normalised to ^{132}Xe (Crabb and Anders, 1981). These noble gases are usually chosen to represent the so-called "subsolar" noble gas component of unknown origin that resides in meteoritic silicates. Independent measurements in both of our laboratories yield similar solar-like noble gas patterns in D'O glass (Fig. 6), thus making an experimental artifact highly unlikely. In contrast to the glass, the bulk samples show element patterns that are highly fractionated relative to that of the Sun, favouring the heavy elements. Such patterns are typical for meteorites as indicated by the bulk composition of the CV3 chondrite Grosnaja (Busemann et al., 2000).

4. Discussion

4.1. The origin of the glass in D'Orbigny

Our most surprising observation is the probable presence of solar-like noble gases in D'O glass that are not accompanied by detectable solar gases in the bulk (Figs. 1 and 6). In the following, we discuss possible trapping mechanisms and argue that these solar gases originate from the interior of the APB. The normal origin of solar gases in meteorites is the exposure to solar wind in the regolith of the parent body. However, in the case of D'O glass, this can be excluded, because D'O is not reported to be a breccia. Furthermore, it is inconceivable that the crystalline bulk material completely lacks solar wind, whereas the

glass retained significant amounts of the solar gases. Hence, the solar gases were most likely trapped from primordial reservoirs present during the formation of the glass. Two mechanisms are known to form glass and incorporate noble gases:

(i) Impact-induced shock that causes partial melting of the impactor or surficial material. If an atmosphere or nebula gas is present, rapidly cooling melt can form glass that contains some of the ambient gas. This occurred on Mars—some of the Martian meteorites contain glass that trapped gas from the ancient and more recent Martian atmosphere (see, e.g., Bogard et al., 2001). It also took place during the formation of tektites on Earth (e.g., Mizote et al., 2003).
(ii) Magma that rises from lower layers of a planetary body through the crust. Eruptive magmatism requires sufficient heat and significant amounts of interior volatiles (e.g., Wilson and Keil, 1991). If the hot magma reaches the cool surface (or the ocean floor), the quenched material is able to retain volatiles. This is observed for terrestrial basalts that formed at mid-ocean ridges or ocean islands (e.g., Graham, 2002). Noble gases in these basalts led to the belief that the interior of the Earth contains solar-like He and Ne.

We suggest that an igneous process similar to the second scenario was responsible for the incorporation of solar-like noble gases into D'O glass. Wilson and Keil (1991) showed that explosive pyroclastic volcanism can take place on small bodies (radius up to ~100 km) within the first 10 Ma after their formation. Even low concentrations of volatiles in the magma are sufficient to furnish the melt with velocities even above the escape velocity of the small asteroids. The old formation ages of the angrites (Table 1) likely date rapid cooling of the APB after the end of this early, active phase.

During crystallization D'Orbigny experienced the addition of "multiple magma batches," either due to new magma from the interior of the APB or because of simple stirring of the flowing magma (Mittlefehldt et al., 2002). Evidence for volatiles accompanying magmatism on the APB was also found by McCoy et al. (2003), who attribute the large vesicles in the angrites D'O and S99 to volatiles (mainly CO_2) in a magma that was rapidly rising through a dike and cooled close to the surface. Therefore, the abundant glass in D'O may simply represent new magma that filled already existing empty spaces (Varela et al., 2003) or cooled more rapidly than the adjacent crystalline material. Mn–Cr systematics show that bulk and glass formed within 0.3 Ma (Glavin et al., 2004). This implies that either the new magma caused a resetting of the Mn–Cr clock of the pre-existing crystalline host material or that the crystalline material solidified shortly after the glass. The former appears less likely, because D'O minerals including olivines are highly zoned, which would probably be destroyed by any event that causes the resetting of the Mn–Cr system (Mittlefehldt et al., 2002).

If rising volatiles from the interior of the APB formed the vesicles, these volatiles may have contained solar-like noble gases that originated from the interior. D'O glass has been reported to contain small bubbles (Varela et al., 2003), which thus are the most probable site where the trapped solar noble gases were incorporated. Marty and Lussiez (1993) showed by comparing olivine and glass separates from natural terrestrial basalts that during partial melting the noble gases largely dissolve in the melt (upper limits for olivine–melt partitioning for He and Ar are 0.008 and 0.003, respectively). This could explain why the crystalline D'O bulk material does not contain solar noble gases. Most of the noble gases in the glass should reside in vesicles, because of the generally poor solubility of noble gases in melt.

Relative solubility of the light and heavy noble gases depends on the concentrations of the major volatiles H_2O and CO_2 (Nuccio and Paonita, 2000) and SiO_2 (Pinti et al., 2004). Therefore, one might argue that the solar-like element pattern in D'O glass is due to an increased solubility in the angritic melt of the light relative to heavier elements of originally typical meteoritic noble gases ("Q-gases"). An enrichment of He and Ne relative to the heavier elements and air is indeed observed in tektites (Mizote et al., 2003). However, the ^{4}He abundance can be entirely attributed to radiogenic ^{4}He (Section 4.6), which excludes significant ^{4}He contributions from Q-gas. Similarly, the *solar* Ne isotopic composition in the glass with $^{20}Ne/^{22}Ne \approx 11.9$ (Fig. 1) most likely does not imply the presence of over-abundant Q-gas, which typically shows $^{20}Ne/^{22}Ne$ ratios $\leqslant 10.7$ (Busemann et al., 2000).

4.2. Solar noble gases in the interior of a small planetary body

Our results suggest that the APB might be, next to Earth and Mars, a further planetary body in the inner solar system of which the interior contains solar noble gases. The APB is assumed to be small (50–100 km, Nyquist and Bogard, 2003). This is not sufficient to gravitationally attract a thick proto-atmosphere from which solar noble gases including He could have been trapped in a magma ocean. Such a scenario has been suggested for the Earth (Mizuno et al., 1980; Porcelli et al., 2001). Note that the Earth is heavier than the APB by the order of 10^5. A pressure of ~100 bar has been inferred for the Earth's atmosphere at this stage. This is clearly ruled out for the APB. Ambient nebula gas may have been present during the very early formation of D'O (Table 1). The nebula is assumed to be removed within ~1–20 Ma (Podosek and Cassen, 1994; Feigelson and Montmerle, 1999; Wadhwa and Russell, 2000). However, the low pressure of the solar nebula ($\sim 10^{-4}$ bar), the presence of vesicles and bubbles in

D'O, and petrologic considerations (Mittlefehldt et al., 2002; Floss et al., 2003) provide strong evidence for a magmatic process that carried the interior noble gases upwards rather than trapping of nebula gas during condensation to be the most plausible process to explain the trapped solar noble gases.

The presence of solar noble gases in the interior of the small APB implies a trapping mechanism for noble gases in a planetary body that does not depend on its gravitation. The solar noble gases may have been incorporated into the precursor matter of the APB. The most likely mechanism is the irradiation of the angritic precursors with solar wind, because this is known to incorporate solar noble gases which are largely unfractionated (Geiss et al., 1972; Wieler, 1998). Such a mechanism was proposed to explain the light solar noble gases in the Earth (e.g., Podosek et al., 2000; e.g., Tolstikhin and Hofmann, 2005), the "subsolar" Ar–Xe in chondrules of an E chondrite (Okazaki et al., 2001) and the traces of primordially trapped solar noble gases in another E chondrite (Busemann et al., 2003a,b). Other trapping mechanisms that could lead to the incorporation of unfractionated solar noble gases are at present not known. Adsorption on cold siliceous or carbonaceous matter causes significant elemental and isotopic noble gas fractionation, particularly for He and Ne, relative to solar composition (e.g., Pepin, 1991; Wieler et al., 2006).

The observations imply that the dissolution of a thick proto-atmosphere in a magma ocean is not necessary to explain solar-like noble gases in the bodies of the inner solar system. The proposed irradiation of the material that subsequently formed the very old APB requires a fast removal of the nebular gas and dust within the first 5–10 Ma after formation of the CAIs, or the origin of the precursor materials from less protected regions above the nebular mid plane. This has been suggested to explain the solar-like noble gas composition of the atmosphere of Venus (Sasaki, 1991).

4.3. Cosmic-ray exposure ages for Sahara 99555 and D'Orbigny bulk

The CRE ages of bulk S99 and D'O are given in Table 9. The CRE ages based on the "physical model" (LE, Section 3.1) are higher than those based on the "empirical model" (EM) by ~50% for D'O bulk and ~30% for S99. The ages obtained with both models for D'O glass are in good agreement (Table 9). In the following, we will use the ages obtained with the EM model, because this model also covers Ar–Xe and the LE model implies an unreasonably small pre-atmospheric radius for D'O (see Section 3.1). All implications discussed in this work also would remain valid with the higher ages obtained by the LE model.

We obtained error-weighed mean ages of (6.8 ± 0.3) Ma for S99 and (11.9 ± 1.2) Ma for D'O. As for D'O glass, the ages deduced from the various systems agree reasonably well with each other, indicating that neither S99 nor D'O (Fig. 7) suffered diffusive loss during thermal processing.

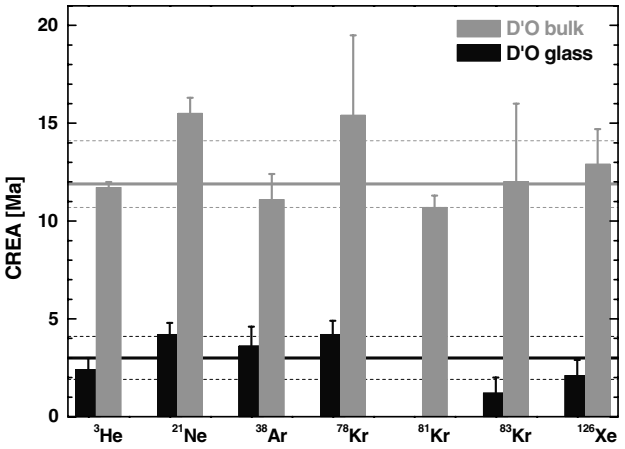

Fig. 7. The cosmic-ray exposure ages for D'O bulk and D'O glass differ by ~9 Ma, with the glass being exposed to cosmic rays for a shorter period. The glass has been reported to have been introduced into the pre-existing matrix material (Varela et al., 2003). A pre-exposure of the bulk relative to the glass is unlikely, because the Mn–Cr formation ages for the bulk and the glass are within 0.3 Ma identical (Glavin et al., 2004). The very similar CRE ages obtained for both samples from different systems including the most volatile light isotopes ^{3}He and ^{21}Ne exclude significant diffusive losses.

4.4. Cosmic-ray exposure history of the angrites

The comparison of our results with CRE ages obtained for the other angrites (Table 9) indicate that all angrites except for L86 and N16 most likely originate from different ejection events. S99 and A88 show similar ages, though the values do not agree within their uncertainties. The lower limit given for the age of L87 in combination with the observation of significant loss of $^{4}He_{rad}$ (Eugster et al., 1991) of course does not exclude that L87 originate from the same ejection event as A88, S99 or D'O.

However, the angrites L87, A88, S99, D'O and N16, which might originate from very similar magmas (Floss et al., 2003; Mikouchi et al., 2003) may have been ejected during a single impact event, but were pre-exposed to cosmic rays close to the surface for various time intervals. Such pre-exposure on the APB close to the surface agrees well with the quenched character of these meteorites and their very fast cooling, which has occurred, in the case of S99, within 1 m from the surface (Mikouchi et al., 2000, 2003).

AdoR and L86 show different, distinctly higher CRE ages, emphasizing the distinct composition and petrogeneses of these angrites (Mittlefehldt et al., 2002). The spread of the CRE ages suggests at least five ejection events (Table 9). Complex irradiation histories, such as that suggested for AdoR and possibly also L86 (Hohenberg et al., 1991) would lower this number. However, there is no compelling evidence for complex irradiations in S99 and D'O (Section 4.10).

4.5. The cosmic-ray exposure and formation ages of D'Orbigny glass

An interesting observation is the discrepancy between the CRE ages of D'O bulk and glass. The average bulk CRE age is (11.9 ± 1.2) Ma and is apparently 9 Ma higher than that of the glass, which is only (3.0 ± 1.1) Ma (Table 9, Fig. 7). The actual difference would be ~18 Ma, because the ages were calculated for a 4π-exposure to cosmic rays in space, after ejection on the APB. However, the divergence in the ages must be the result of processes that occurred on the APB in a 2π-exposure scenario, because after ejection D'O bulk and glass inevitably experienced the same exposure to cosmic rays.

At present, the reason for these variations is unclear. Most likely, this difference is the result of abundant secondary, gas-free glass in our aliquots, which lowers the apparent exposure age of D'O glass. This is not easy to achieve, because gas-free fractions of ~85% would be necessary in *both* glass separate aliquots that we independently analyzed in two laboratories (94 and 20 mg, respectively, with grains of ~0.05–2 mg). Unfortunately, the ^{81}Kr–Kr age for D'O glass, which is independent from the gas concentrations, could not be measured due to too low ^{81}Kr abundance. Secondary glass could have been easily formed during the entry of D'O into the terrestrial atmosphere as suggested for "unusual glass" in the eucrite EET 90020 (Garrison et al., 1998). Note that the glass has been selected from various regions of the meteorite and includes loose grains that have been found in the meteorite's case (M.E. Varela, pers. communication). This interpretation of secondary gas-free glass in the analysed glass batches based on the CRE ages is supported by comparable discrepancies found in the U/Th–He (Section 4.6) and possibly the ^{244}Pu–Xe systematics (Section 4.9).

It is clear from the following reasons that the glass in D'O, which carries the noble gases, is not the result of a more recent event that occurred much after the formation of the bulk of D'Orbigny:

(i) The ^{53}Mn–Cr ages of D'O bulk and glass reveal that both were almost simultaneously formed, within only ~0.3 Ma (Glavin et al., 2004). The glass was formed from a melt of primary origin and was not introduced from an external source after the rock had formed. The possibility that the Mn–Cr clock of the precursor material of the glass remained undisturbed during the event that introduced glass and vesicles, while the noble gases were completely released, appears highly unlikely. The closure temperature for the Mn–Cr system in basalts is near the solidus of 1380 K (Nyquist and Bogard, 2003). Accordingly, the glass-forming event must have occurred at temperatures below ~1100 °C. Analyses of the angrite AdoR showed, however, that only Xe due to spallation of Ba is released below 1200 °C at laboratory time scales, whereas Xe produced from the rare earth elements resides in more refractory minerals (Hohenberg, 1970). Hence, the ^{126}Xe-CRE age of D'O glass should be larger than the other CRE ages, which is not the case (Fig. 7).

(ii) Old Pb–Pb ages of the glass support the view that it is not produced during a late planetary event (Table 1).

(iii) This study shows that the glass carries excess ^{129}Xe from the decay of short-lived ^{129}I ($T_{1/2} \sim 16$ Ma) (Section 3.4). This is the first detection of fossil ^{129}I in angrites, in agreement with the presence of several other, once live short-lived radionuclides (see introduction and Table 2).

(iv) The glass contains Xe_{fiss} from the presence of once live ^{244}Pu ($T_{1/2} \sim 80$ Ma). Initial single grain analyses indicate that both Xe_{fiss} and Xe_{sp} were produced in situ (Busemann et al., 2005).

These arguments exclude a pre-exposure of the bulk for ~20 Ma close to the surface of the APB or a complete degassing of the glass, 20 Ma after the beginning of the exposure of the bulk material. Furthermore, an early 20 Ma pre-exposure to cosmic rays of D'O bulk contradicts the formation of the APB and the glass only ~5–10 Ma after the CAIs (Table 1). These discrepancies can only be reconciled by a cosmic-ray intensity during the first 10 Ma of the solar system that was two orders of magnitude larger than at present and an already dissipated nebula when the angrites were formed and became irradiated.

The difference in the CRE ages of D'O bulk and glass is not the result of diffusive gas loss exclusively in the glass after the ejection from the APB: All ages obtained from the various spallogenic isotopes in both glass samples agree well with each other (Fig. 7). Diffusive gas loss from the glass would hamper the retention of light ^{3}He much more than that of, e.g., ^{126}Xe.

4.6. U/Th–He and K–Ar retention ages

Gas-retention ages date events that occurred to D'O and S99 after crystallization. These events include late impact or other thermal activity on the APB or during transfer to Earth. The APB appears remarkably undisturbed, as proven by the old ^{4}He-retention ages of D'O and S99 of (4.2 ± 0.6) and (4.6 ± 0.6) Ga, respectively. Some U/Th–He and K–Ar retention ages for other angrites support this view (Table 10). However, Garrison and Bogard (2003) concluded from their results on L86 and D'O that angrites may be not dateable with the K–Ar system due to weathering and loss of radiogenic Ar. This is also suggested by our work on bulk D'O and S99 (Table 10), which is discussed in the following.

The K–Ar systematics for angrites is difficult to assess, because the Ar-retention age frequently appears to be younger than the respective He-retention age (e.g., Eugster et al., 1991). This has been observed for AdoR (Ganapathy and Anders, 1969; Müller and Zähringer, 1969), L86

(Eugster et al., 1991) and S99 (Bischoff et al., 2000). We observe this paradoxal behaviour also for S99 and D'O. Their Ar-retention ages are <2 Ma (Table 10). Possibly, the U/Th–^{4}He retention ages of S99 and D'O could be in the range of 4.2–4.6 Ga, due to ^{4}He from known short-lived radionuclides—or yet undetected species—that compensate loss of ^{4}He originating from the decay of U and Th. However, contributions from the extinct α-emitters ^{146}Sm, ^{244}Pu, and ^{247}Cu are <0.6% for both S99 and D'O, and hence cannot account for this extra ^{4}He. For the estimate, we assumed the complete retention of ^{4}He and conservative branching into ^{4}He decay of 100%, and used the initial ratios $(^{146}Sm/^{144}Sm)_0 = 0.008$ (Prinzhofer et al., 1992), $(^{244}Pu/^{150}Nd)_0 = 1.6 \times 10^{-3}$ (Lugmair and Marti, 1977), and $(^{247}Cm/^{144}Nd)_0 = 2.9 \times 10^{-6}$ (Stirling et al., 2005). Similarly, a contribution <3% was estimated for AdoR (Störzer and Pellas, 1977).

Otherwise, Ar often resides in less retentive minerals than He. The most compelling reason for the young K–Ar ages, however, might be terrestrial weathering, because K is rare in angrites and thus easily affected by terrestrial contamination (Eugster et al., 1991). To obtain nominal K–Ar ages of ~4.56 Ga, the primordial K content must have been as low as ~1 (D'O) and 8 μg/g (S99). Most of the measured K (Tables A1 and A2) would be terrestrial contamination and hence the K–Ar ages strongly affected.

For D'O glass, we determine an apparent ^{4}He-retention age of only 0.8 Ga (Table 10), which is an upper limit due to additional solar ^{4}He$_{tr}$ (see Section 3.2). This is in contrast to the D'O bulk U/Th–^{4}He age of 4.2 Ga. Inhomogeneities or contamination must have led to an overestimation by factors of ~10 of the U and Th content in D'O glass to explain its low ^{4}He-retention age. This is unlikely in view of the rather uniform concentrations found by different laboratories (Table A2). Therefore, most likely the low He-retention age is, in agreement with the low CRE age of D'O glass (Section 4.5), due to an admixture of ~90% gas-free glass. Contrastingly, the Ar-retention age of D'O glass is, within the large uncertainty, in agreement with a formation 4.56 Ga ago. However, believing that most of the glass is of secondary origin, we assume that this age is, as that of D'O bulk, affected by terrestrial K contamination. This is supported by the enormously varying K concentrations in D'O glass (Table A2).

4.7. Fission xenon retention ages of Sahara 99555 and D'Orbigny bulk

Fig. 8 shows the ^{244}Pu–^{136}Xe ages for angrites obtained in this work and from literature data (Munk, 1967; Hohenberg, 1970; Lugmair and Marti, 1977; Eugster et al., 1991; Hohenberg et al., 1991; Weigel et al., 1997). We performed identical procedures for all data sets to decompose Xe into Xe$_{fiss}$ and Xe$_{sp}$ and determine the ages (Section 3.4). The usefulness of the ^{244}Pu–^{136}Xe

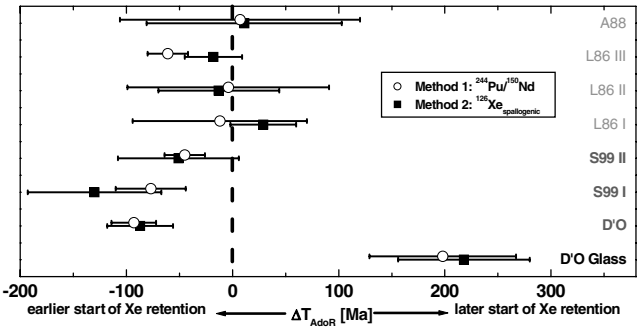

Fig. 8. The ^{244}Pu–^{136}Xe retention ages of angrites relative to AdoR as determined via ^{150}Nd (method 1, see Section 4.7) and ^{126}Xe$_{sp}$ concentration (method 2). The generally similar ages obtained from both methods indicate that Nd and Pu in the angrites are homogeneously distributed. Most angrites plot around time "0" defined by the absolute Pb–Pb age of AdoR (Table 1), which implies a formation of the angrites around 4.558 Ga ago. The vesicular angrites S99 and D'O bulk show apparent ages that are 50–100 Ma before AdoR. This is probably due to the addition of parentless fission Xe, rather than geochemically incoherent Nd and Pu. D'O glass shows a much smaller ^{244}Pu–^{136}Xe retention age. The reason for this remains unclear. (References for other angrite data: Fig. 2).

chronometer is controversial, because of the uncertain geochemical behaviour of Pu. The mother nuclide ^{244}Pu is extinct and Pu has no stable isotope. There are two possibilities in use to replace the missing stable reference isotope:

(i) The "canonical" method uses ^{150}Nd as proxy for the primordial ^{244}Pu concentration. Neodymium and Pu are thought to be geochemically coherent (Lugmair and Marti, 1977; Boynton, 1978; Jones, 1982). The initial solar system ratio $(^{244}Pu/^{150}Nd)_0$ of 1.6×10^{-3} was obtained from AdoR (Lugmair and Marti, 1977). The coherence of Pu and Nd, however, and thus the entire method has been questioned (Crozaz et al., 1989; Hohenberg et al., 1991; Crozaz, 1994; Ebihara et al., 2000). Furthermore, reliable age information can be obtained only if ^{150}Nd and ^{136}Xe$_f$ are homogeneously distributed in the sample, because both elements cannot be measured by the same technique.

(ii) The second method circumvents the problem of potential elemental inhomogeneities by using ^{126}Xe$_{sp}$ as a proxy for Nd (Hohenberg et al., 1991). Only the less error-prone isotopic ratio ^{136}Xe$_{fiss}$/^{126}Xe$_{sp}$ is thus needed, which can be obtained in a single aliquot. The original approach uses the Xe$_{sp}$ isotopic composition to determine the fraction of Xe$_{sp}$ that originates from Ba on the one hand and the light rare earth elements (REE) La, Ce and Nd on the other, assuming that the actual proportions of the latter do not vary significantly. A modified method (ii) (Shukolyukov and Begemann, 1996) applies a constant ratio for the production rates of Xe$_{sp}$ from Ba and the REE (Hohenberg et al., 1981). This procedure was

successfully applied to eucrites. Generally, the obtained ages agreed well with each other and other chronometric systems, showing that Pu and Nd in eucrites are indeed coherent within ~15%, hence proving the reliability of method (ii) (Shukolyukov and Begemann, 1996).

We applied both the first and the modified second method. The relative ages, calculated relative to AdoR, are compiled in Fig. 8. Both methods give generally very similar results, showing that potentially inhomogeneously distributed Nd and Pu in angrites do not affect the results, because method (ii) only rests on Xe isotope ratios. The same has been concluded for the eucrites. Most angrite ages scatter around the reference point $\Delta T_{AdoR} = 0$ -Ma, which relates the relative ^{244}Pu–^{136}Xe ages to an absolute time scale. The absolute Pb–Pb age of AdoR is 4.5578 Ga (Table 1).

S99 and D'O bulk show apparent retention ages of ~100 Ma before the closure time of AdoR. This appears impossible and indicates either the presence of additional Xe_{fiss} or geochemically incoherent Nd and Pu. The time difference between S99/D'O and AdoR is about one half-life of ^{244}Pu (80 Ma). Therefore, the initial $(^{244}Pu/^{150}Nd)_0$ in S99 and D'O bulk must have been $\sim 3 \times 10^{-3}$ rather than 1.6×10^{-3} to achieve agreement of the ages for bulk S99, D'O and AdoR. Interestingly, phosphates from the Forest Vale chondrite yield a very similar initial $^{244}Pu/^{150}Nd$ ratio of $\sim 3.4 \times 10^{-3}$ (Lavielle et al., 1992). In summary, our analyses of S99 and D'O as well as results from the literature may imply that Nd and Pu are geochemically incoherent. However, this conclusion is difficult to reconcile with the geochemically *coherent* behaviour of Nd and Pu in other angrites that are supposed to originate from the same magma (see introduction).

4.8. Bulk parentless fission xenon and fission xenon isotopic composition

Our results may still support the assumption of geochemically coherent Pu and Nd, if S99 and D'O contain "parentless" Xe_{fiss}, acquired from gaseous reservoirs during planetary processing or produced in situ from now extinct progenitors other than ^{244}Pu and ^{238}U. Potential parent nuclides are ^{235}U and ^{247}Cm (both via n-induced fission), ^{248}Cm (spontaneous fission plus α-decay to ^{244}Pu), and the daughter nuclides of ^{247}Cm (spontaneous fission). The putative extra Xe_{fiss} amounts to roughly half of the total Xe_{fiss} in S99 and D'O. Hence, the isotopic composition may give hints on the origin of this additional Xe_{fiss}. Fig. 9 shows the data for angrites available in the literature and from this work corrected for Xe_{sp} (Section 3.4). For comparison, other fission Xe components are plotted. The pure fission endmember composition in the angrites can be inferred by extrapolating the trapped Xe composition through the respective data points towards $^{130}Xe/^{136}Xe = 0$. All *bulk* angrites show fission Xe

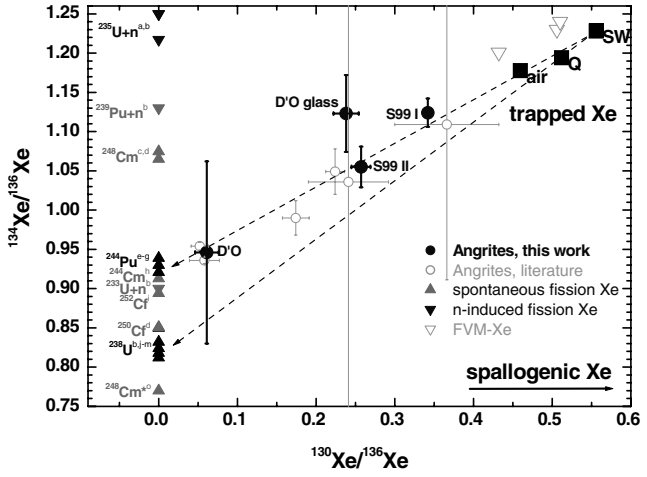

Fig. 9. The isotopic composition of fission Xe in angrites shows the presence of now extinct ^{244}Pu. Most data plot exactly on the mixing line between ^{244}Pu–Xe and trapped Xe. D'O glass may indicate the additional release of an isotopically different fission Xe component. However, the uncertainty—mainly due to the blank correction—is too large to be conclusive. References for the fission Xe components: [a]Fleming and Thode (1953), [b]Hyde et al. (1964, and references therein), [c]Leich et al. (1977), [d]Srinivasan and Flynn (1980), [e]Alexander et al. (1971), [f]Lewis (1975), [g]Hudson et al. (1982), [h]Flynn et al. (1972), [i]Srinivasan et al. (1969), [j]MacNamara and Thode (1950), [k]Wetherill (1953), [l]Hebeda et al. (1987), [m]Eikenberg et al. (1993), [o]Rao and Gopalan (1973), *predicted composition. FVM-Xe: Marti et al. (1989). See Figs. 1 and 2 for further references.

compositions between those of ^{244}Pu- and ^{238}U-fission, indicating that live ^{244}Pu was present during the crystallisation of all angrites and abundant other fission Xe components are not present.

Given the comparable half-lives of ^{248}Cm (0.34 Ma) and ^{26}Al (0.72 Ma), which was definitely present in S99 and D'O (Table 2) and the early formation of the angrites, it is possible to speculate about the presence of ^{248}Cm. The in situ decay of potentially once present ^{248}Cm would lead to a cumulated fission Xe isotopic composition that is significantly different to that of ^{244}Pu–Xe, although 91.6% of ^{248}Cm decays to ^{244}Pu, because the fission branching ratio for ^{244}Pu is only ~0.12% (Ekström and Firestone, 1999). $^{136}Xe_{fiss}$ from ^{244}Pu would deliver only ~1–2% of the total ^{248}Cm-induced $^{136}Xe_{fiss}$, assuming ^{136}Xe fission yields of 5.6% for ^{244}Pu and 6% for ^{248}Cm. However, the extrapolation of the bulk S99 and D'O data points ends very close to ^{244}Pu–Xe. This excludes significant contributions from spontaneous fission of ^{248}Cm (or any n-induced fission). Lavielle et al. (1992) determined an upper limit for $^{248}Cm/^{244}Pu$ in the early solar system of 1.5×10^{-3}. We will not calculate the initial solar system value here, because it is not clear whether ^{248}Cm indeed strictly chemically follows ^{244}Pu (Boynton, 1978). However, in conclusion, in situ produced fission Xe from the decay of ^{248}Cm is not the reason for the too old ages found for S99 and D'O. The spontaneously fissioning daughters of ^{247}Cm (^{243}Am and ^{239}Pu) show also too small branching ratios (3.7×10^{-9}% and 3.0×10^{-10}%, respectively, Ekström and

Firestone, 1999) to be responsible for the production of the excess Xe_{fiss}.

With the modified version of method (ii), we determined for L86 III (data from Hohenberg et al., 1991) a Xe closure time of 18 ± 27 Ma *before* AdoR (Fig. 8). Using their original method (ii), Hohenberg et al. found an age of ~60 Ma *after* AdoR, assuming a constant initial Pu/Nd in both angrites, and suggested that Pu and Nd may not be geochemically coherent. The discrepancy between their and our new age is not the result of distinct results of the decomposition of the measured Xe isotopic composition, because Hohenberg et al. and this work yield rather similar values for ^{244}Pu–Xe_{fiss} (11.5 vs. 12.7×10^{-12} cm^3/g) and total $^{126}Xe_{sp}$ (2.12 vs. 2.14×10^{-12} cm^3/g). However, the spallogenic Xe_{AdoR}/Xe_{REE} ratio of 1.91 obtained from the Xe_{sp} isotopic composition (Hohenberg et al., 1991) divided by the production rate ratio $P_{AdoR}/P_{REE} = 1.82$ (Hohenberg et al., 1981) implies a Ba/(La + Ce + Nd) ratio of ~1.1. Table A3 gives a Ba/(La + Ce + Nd) ratio of ~0.65 for AdoR. In contrast, the Ba/(La + Ce + Nd) ratio as used in this work for all other angrites is 2.6 (Table A3). This may indicate that the Ba to REE ratio in L86 is varying by a factor of ~2 or that the isotopic composition of Xe_{sp} may not be very suitable to precisely determine the Ba/REE ratio in angrites, because of the small variation between the isotopic compositions of Xe_{sp} from Ba and REE, respectively, compared to the generally large difference of Xe_{sp} and Xe_{tr}. Note that even the data from single glass grain measurements, obtained with a high-sensitivity mass spectrometer (Busemann et al., 2005), could not resolve the two spallogenic compositions.

Analyses of the eucrites Ibitira and Pasamonte indicate a start of Xe retention up to 35 Ma before that of AdoR (Shukolyukov and Begemann, 1996). Interestingly, Ibitira is a vesicular achondrite (McCoy et al., 2002). This allows us to speculate that those ^{244}Pu–^{136}Xe ages measured by Shukolyukov and Begemann, which are apparently older than that of AdoR or the Pb–Pb age of Ibitira of (4.560 ± 0.003) Ga (Manhès et al., 1987), may indeed be the result of parentless fission Xe. Abundant excess ^{129}Xe from the decay of ^{129}I is present in Ibitira (Chen and Wasserburg, 1985), which is in contrast to most other eucrites (Shukolyukov and Begemann, 1996). This may support the view that Ibitira is a eucrite that contains additional Xe of inherited volcanic origin (Shukolyukov and Begemann, 1996), similar to the angrites discussed here. The solar-gas-rich howardites Bholghati and Kapoeta were reported to show excess fission Xe and excess ^{129}Xe, and may have acquired outgassed parentless fission Xe during their residence in the regolith, as observed for Ar in lunar samples (Swindle et al., 1990). To conclude, the Pu-fission Xe systematics in angrites discussed here and found earlier for certain eucrites are consistent with the presence of parentless fission Xe inherited from the interior of their parent bodies.

4.9. Fission xenon retention age of D'Orbigny glass

D'O glass yields a Xe-retention age that is much younger than that of the bulk, ~200 Ma after the closure time of AdoR and ~300 Ma after that of bulk D'O (Fig. 8). Since late resetting is excluded by the Mn–Cr systematics (Table 1), this possibly reflects a very low initial $(^{244}Pu/^{150}Nd)_0$ in D'O glass of only 3.5×10^{-4}. The chemical composition of the glass, however, is remarkably similar to that of the bulk, which suggests only little fractionation during the melting of D'O bulk material (Tables A1 and A2). Hence, one might argue that the younger Xe-retention age of D'O glass is, as discussed above, an artefact due to dilution with secondary, gas-poor glass. Using method (i) and assuming a dilution with ~90% of gas-free glass would indeed accommodate the Xe-retention age of the glass with that of the bulk, However, method (ii) relies only on the isotopic *ratio* of spallogenic and fissiogenic Xe and does not change due to dilution. This excludes dilution to be the only reason for the discrepancies. Thus the Xe-retention age of D'O glass remains mysterious. Detailed Xe analyses of single D'O glass grains in collaboration with the University of Manchester will shed more light on the problem.

4.10. Neutron effects in D'Orbigny and Sahara 99555?

Neutron (n) effects can be observed in meteorites if their pre-atmospheric size was large enough and secondary neutrons produced by cosmic rays became thermalized within the meteoroid, or if the meteoritic material, which once resided for considerable time within the sufficiently shielded uppermost layers of an atmosphere-less parent body. The $(^{22}Ne/^{21}Ne)_{sp}$ ratios (Section 3.1) of D'O and S99 imply only low shielding in rather small meteoroids. However, the angrites formed in surface-near regions of the atmosphere-less APB (see introduction), which may allow the build-up of sufficiently large neutron fluences. D'O bulk and S99 do not show significant excesses of ^{80}Kr, ^{82}Kr and ^{128}Xe within uncertainty. In contrast, D'O glass exhibits small excesses in ^{80}Kr $(2.0 \pm 0.7 \times 10^{-12}$ cm^3/g) and ^{82}Kr $(0.7 \pm 0.3 \times 10^{-12}$ cm^3/g) due to n-capture on bromine (Fig. 5). The lack of similar excesses visible in the surrounding D'O bulk material may suggest that the glass simply contained more abundant volatiles including bromine than the crystalline silicates, which is in agreement with the ^{129}I-induced excess in ^{129}Xe and the solar noble gases found solely in the glass (Section 3.5).

4.11. The D'O glass fission xenon isotopic composition

Jagoutz et al. (2003) observed in the glass of D'O large ^{235}U enrichments of ~2% relative to ^{238}U and terrestrial composition. The authors attributed this to the decay of once live ^{247}Cm, which decays via three α-decays into ^{235}U. The Xe_{fiss} isotopic composition in D'O glass may

reflects this enormous variation in the $^{235}U/^{238}U$ ratio. Indeed, the Xe isotopic composition in D'O glass plots slightly off the mixing line between ^{244}Pu- and ^{238}U-fission Xe (Fig. 9). This could indicate an additional fissiogenic Xe component, although the uncertainty, mainly caused by the large blank subtraction, is substantial, and single glass grain analyses do not support the presence of any other fission Xe component than ^{244}Pu–Xe (Busemann et al., 2005). This Xe_{fiss} could have been produced by additional n-induced fission of ^{235}U or ^{247}Cm, although there is no compelling evidence for thermalised neutrons (Section 4.10). As observed on the moon, an abundant cosmic-ray-induced flux of thermalised secondary neutrons probably could have penetrated the uppermost meters of the surface.

How long had the glass experienced an exposure to thermal neutrons to show an n-induced excess of $^{136}Xe_{fiss} \sim 5.6 \times 10^{-12}$ cm^3/g? This excess is calculated assuming that the glass formed 4.56 Ga ago ($\Delta t = 0$, Fig. 8), and is corrected for 80% secondary, gas-free glass. We adopted maximum and minimum fission rates of 3.5 and 1.0 ^{235}U atoms/(s × g), respectively, as deduced for the moon (Woolum and Burnett, 1975) and assumed that the glass was exposed instantaneously after formation. The U concentration of 0.10 μg/g is given in the appendix. Our rough calculation yields 320 and 1120 Ma, respectively. These periods are unreasonably long and exclude that the observed excess originates from ^{235}U. Moreover, the crystalline material of D'O that surrounded the glass did not acquire a similar dose of neutrons. An early irradiation of *proto*-planetary matter with a high n flux has been suggested to explain the isotopically highly anomalous fission Xe in Forest Vale chondrite metal (''FVM'', Marti et al., 1989). The FVM-Xe composition (Fig. 9) indeed implies, within large errors, n-induced fission of ^{235}U.

As described above, the daughter nuclides of ^{247}Cm (^{243}Am and ^{239}Pu) decay only negligibly via spontaneous fission. ^{247}Cm itself splits only by thermal n, with a high fission cross-section (~80 barn, Pfennig et al., 1998). The n-induced fission Xe composition of ^{247}Cm is unknown and cannot be predicted by systematic considerations. For example, the attempt to a-priori estimate the spontaneous fission Xe composition of ^{248}Cm (Rao and Gopalan, 1973) failed. This can be seen by the comparison of the predicted composition (Fig. 9, marked with ''*'') and the measured values (Leich et al., 1977; Srinivasan and Flynn, 1980). The distribution of fission Xe components (Fig. 9) shows that neither odd/even distinctions nor variations in mass or the decay mechanism (spontaneous vs. neutron-induced fission) allow any prediction due to unknown fine-structure effects.

Stirling et al. (2005) gave an upper limit for the initial $(^{247}Cm/^{144}Nd)_0$ in the solar system of 2.9×10^{-6}. Assuming that Cm and Nd are geochemically coherent, a Nd concentration of 5.1 μg/g (Table A2), fission rates as given above for ^{235}U, and a $^{136}Xe_{fiss}$ yield of 6%, we would expect merely $\sim 0.00004 \times 10^{-12}$ cm^3/g ^{247}Cm-induced $^{136}Xe_{fiss}$. This is ~0.002% of the totally measured fission Xe. Neutron-induced fission of ^{247}Cm hence does not measurably affect the Xe_{fiss} isotopic composition.

In view of the results discussed above and the large uncertainty of the Xe isotopic composition in D'O glass, the presence of an additional Xe_{fiss} component due to n-induced fission of ^{235}U or ^{247}Cm is highly unlikely. Results from single grain analyses of D'O glass must be awaited to conclusively prove or disprove the presence of another Xe_{fiss} component.

5. Conclusions

We determined and discussed the noble gas contents of bulk samples of the angrites Sahara 99555 and D'Orbigny as well as glass from D'Orbigny. Here we summarize our most important findings:

1. D'O glass contains abundant trapped noble gases of most probably solar composition. This is visible in the trapped elemental and Ne isotopic composition. The trapped solar component shows a $^{20}Ne/^{22}Ne$ ratio of $\sim 11.9 \pm 0.3$. The solar gases most likely originated from the APB interior and were incorporated from rising volatiles in the rapidly forming glass. The crystalline bulk material of S99 and D'O formed too slowly to trap significant amounts of noble gases.
2. D'O glass shows excess ^{129}Xe from the decay of once live short-lived ^{129}I. This is the first evidence for formerly live ^{129}I reported for angrites. The bulk samples of D'O and S99 do not show ^{129}Xe excess.
3. The presence of solar gases and fossil ^{129}I in the interior of the APB shows that the APB did not experience complete devolatilization (Prinz and Weisberg, 1995) and that the precursors of the APB contained volatiles. Hints on n-induced excess of $^{80,82}Kr$ in the glass of D'O produced on Br supports this view.
4. The cosmic-ray exposure ages of S99 and D'O are (6.8 ± 0.3) Ma and (11.9 ± 1.2) Ma, respectively, in agreement with earlier analyses (Bischoff et al., 2000; Kurat et al., 2004). The seven angrites analysed so far sampled angritic surface material in at least five ejection events. S99 and D'O bulk D'O show evidence for a simple exposure to cosmic rays. D'O glass exhibits consistently lower CRE ages than the bulk material of (3.0 ± 1.1) Ma. The reason might be additional, secondary glass in our samples that formed, e.g., during the entry into the Earth's atmosphere. A pre-exposure of the glass relative to the crystallised host can be excluded.
5. The U/Th–He retention ages for S99 and bulk D'O are old and consistent with its old Pb–Pb formation ages (Table 1). The Ar–Ar ages are affected by diffusive loss and insufficiently known K concentrations and are apparently too young compared to the He-retention ages.
6. The ^{244}Pu–^{136}Xe retention ages of most angrites are in agreement with their early formation suggested from other chronometers (Table 1). S99 and D'O, however,

yield apparently too old ages. This is most likely the result of additional, parentless fission Xe that has also been proposed for some eucrites. A geochemical incoherence of Pu and Nd in S99 and D'O seems unlikely, because of the old ages of the other, co-magmatic angrites. There is no evidence for inhomogeneities of the Pu and Nd concentrations in angrites at a tens of mg scale.

7. The apparently too young He and Xe gas-retention ages of the glass in D'O relative to the bulk are in agreement with an addition of secondary, gas-poor glass as suggested to explain variations in the CRE ages. This secondary glass may have formed during the entry of the meteoroid into the Earth's atmosphere. However, the Xe gas-retention age that should be independent of the mass of the sample ("method ii") appears similarly young as the conventionally determined Xe gas-retention age.
8. Fission Xe in D'O glass that can be attributed to the presence of now extinct ^{247}Cm (Jagoutz et al., 2003) cannot be confirmed. The Xe_{fiss} isotopic composition in D'O glass may hint at a n-induced fission Xe component. However, the uncertainty is too large to be conclusive.

Acknowledgments

We thank A. Schaller and H.-E. Jenni for their technical support, M. Schönbächler and A. Case for helpful comments and E. Jagoutz, M.E. Varela and G. Kurat for the D'Orbigny samples. We are grateful to the reviewers U. Ott, B. Marty, an anonymous reviewer and the editor D. Mittlefehldt, who helped significantly to improve this manuscript. This work was supported by the Swiss National Science Foundation. H. B. thanks the Carnegie Institution of Washington.

Associate editor: David W. Mittlefehldt

Appendix A

See Tables A1–A4.

Table A1
Major and trace element concentrations in D'O and S99 (μg/g) important for the determination of CRE ages and retention ages

	D'O			Adopted	S99		Adopted
Ref.	a	a	b,c		d	a	
O	391,717	397,902		427,038 ± 20,000		392,149	406,765 + 10,000
Na	145.6 ± 1.9	109.3 ± 1.5	140 ± 7	132 ± 10	124	122 ± 2	123 ± 10
Mg	39,137			39,137 ± 4000		42,454	42,454 ± 4250
Al	65,627			65,627 ± 5000	68,273	66,156	67,215 ± 5000
Si	179,495			179,495 ± 10,000	180,430	180,430	180,430 ± 10,000
K	137 ± 10[e]	69 ± 15[e]	10[f]	10 ± 5	50	44 ± 19	47 ± 5
Ca	107,204		85,000	96,102 ± 10,000	110,062	107,918	108,990 ± 10,000
Ti	5,335		4,600 ± 690	4,968 ± 400		5455	5455 ± 500
Cr	311 ± 3	262 ± 3	300 ± 15	291 ± 30	280	317 ± 3	299 ± 30
Mn	2,168		1,600 ± 160	1,884 ± 300		2,014	2,014 + 300
Fe	191,996		178,000	184,998 ± 7,000	194,328	179,559 184,500 ± 2,000	186,129 ± 10,000
Ni	56 ± 15	91 ± 15	28 ± 6	58 ± 25		<80	40 ± 40
Rb				2.2 ± 1.5[g]			2.2 ± 1.5[h]
Sr	126 ± 21	142 ± 24	120 ± 24	129 ± 10		107 ± 21	107 ± 21
Y				17 ± 10[g]			17 ± 10[h]
Zr	70 ± 18	66 ± 19	50 ± 8	62 ± 6		n. d.	62 ± 15[h]
Ba	47 ± 18	52 ± 7	42 ± 6	47.0 ± 2.9		45 ± 17	45 ± 17
La	3.56 ± 0.04	3.76 ± 0.04	2.8 ± 0.2	3.37 ± 0.29		3.20 ± 0.04	3.2 ± 0.04
Ce	8.78 ± 0.26	9.18 ± 0.24	8.0 ± 0.6	8.7 ± 0.3		8.41 ± 0.24	8.41 ± 0.24
Nd	n.d.	5.4 ± 2.6	6.0 ± 1.2	5.7 ± 0.3		n.d.	5.7 ± 0.3[h]
Th	0.370 ± 0.040	0.434 ± 0.29	0.33 ± 0.03	0.38 ± 0.03		0.36 ± 0.04	0.36 ± 0.04
U	<0.210	0.116 ± 0.022	0.08 ± 0.02	0.098 ± 0.018		<0.210	0.092 ± 0.026[i]

[a] Mittlefehldt et al. (2002).
[b] Kurat et al. (2001).
[c] Kurat et al. (2004).
[d] Bischoff et al. (2000).
[e] Probably terrestrial contamination (Mittlefehldt et al., 2002).
[f] Garrison and Bogard (2003).
[g] Adopted from D'O glass (Table A2).
[h] Adopted from D'O.
[i] Assuming Th/U = 3.9 ± 1.0.

Table A2
Major and trace element concentrations (μg/g) in D'O glass separates important for the determination of CRE ages and retention ages

Ref.	Glass b	Inclusions type A[a] b	Inclusions type B[a] b	Pockets b	Patches b	With bubbles b	Spheres[a] b	Spheres[a] b	With bubbles[a] b	Patches[a] b	Inclusions[a] b	Pockets[a] b	Bulk glass c	Adopted
O		423,454	397,683	404,448	399,489	387,855	400,349							400,272 ± 40,000
Na													107 ± 1	107 ± 10
Mg		17,247	30,001	25,750	45,831	39,800	46,434						60,000 ± 1,000	37,866 ± 10,000
Al		106,512	60,996	65,098	68,273	62,981	65,451							71,552 ± 10,000
Si		195,738	188,259	189,779	186,039	173,886	186,974							186,779 ± 10,000
K											43	110[d]	18 ± 1	31 ± 15
Ca	102,200	159,019	137,042	152,944	102,201	117,924	99,342	86,815	91,360	94,633	69,125	105,833	136,000 ± 1,000	112,686 ± 25,000
Ti	5,050	9,066	10,565	14,506	2,997	2,997	5,015	4,025	4,482	3,457	3,145	6,313	6,600 ± 8	6,017 ± 2,000
Cr	330	359	479	616	479		547	250	318	520	395	326	236 ± 1	405 ± 100
Mn		1,084	1,878	1,626	2,091	2,633	1,962	1,575	1,624	1,443	3,168	3,633	2,460 ± 5	2,098 ± 800
Fe		84,921	162,847	146,134	185,000	201,324	190,959				161,563	236,667	268,000 ± 1,000	181,935 ± 30,000
Ni	72													72 ± 25
Rb											2.3	2.1		2.20 ± 0.20
Sr	70							88	80	122	46	44	110 ± 1	80 ± 11
Y								14	11	19	12	23	24 ± 1	17.1 ± 2.2
Zr	39							39	34	54	40	88	87 ± 1	55 ± 9
Ba											16	32	23 ± 1	24 ± 5
La	2.1							3.0	2.3	3.2	1.9	3.1	2.7 ± 0.1	2.60 ± 0.20
Ce	6.0							7.6	6.4	6.9	4.5	8.1	6.8 ± 0.3	6.6 ± 0.4
Nd	4.3							5.7	4. 6	5.4	3.9	6.3	5.9 ± 0.2	5.1 ± 0.3
Th	0.25							0.35	0.28	0.54				0.36 ± 0.07
U								0.10	0.08	0.13			0.76/0.123[e]	0.102 ± 0.011

[a] Average of multi-analyses.
[b] Varela et al. (2003).
[c] Floss et al. (2003).
[d] Probably terrestrial contamination, discarded.
[e] Pers. comm., E. Jagoutz (inner/outer parts of a glass grain).

Table A3
Ba, light REE and U concentrations (μg/g) in AdoR (high Ba) and all other angrites (low Ba) adopted for the spallation Xe and ^{238}U fission Xe corrections

Ref.	AdoR a	AdoR b	AdoR c	AdoR d	AdoR e	AdoR f	AdoR g	AdoR g	Adopted	A88 g	D'O h	D'O h	D'O i	L86 e	L86 f	L86 g	S99 h	Adopted
Ba	26.4		21.5		36		30		28 ± 3		47	52	42	48		51	45	47.5 ± 1.5
La		8.3		5.8	6.14		6.9	6.8	6.8 ± 0.4	2.34	3.56	3.76	2.8	3.38		4.66	3.20	3.28 ± 0.24
Ce	20.6	19			19.2		18.9	18.7	19.3 ± 0.3	5.9	8.78	9.18	8	10.1		10.9	8.41	8.5 ± 0.6
Nd	19.8	17		18	16.3	16.1	17.2	16.9	17.3 ± 0.5	4.4		5.4	6		7.762	8.1		6.2 ± 0.6
U							0.14	0.11	0.125 ± 0.015			0.116	0.80			0.15		0.115 ± 0.020

[a] Schnetzler and Philpotts (1969).
[b] Mason and Graham (1970).
[c] Tera et al. (1970).
[d] Ma et al. (1977).
[e] Mittlefehldt and Lindstrom (1990).
[f] Nyquist et al. (1994).
[g] Warren and Davis (1995).
[h] Mittlefehldt et al. (2002).
[i] Kurat et al. (2004).

Table A4
Spallation Xe composition for isotope decomposition, calculated with spectra given by Hohenberg et al. (1981) and Ba and REE concentrations given in Tables A2 and A3

Sample	^{124}Xe	^{128}Xe	^{129}Xe	^{130}Xe ^{126}Xe ≡ 1	^{131}Xe	^{132}Xe	^{134}Xe	^{136}Xe
D'O glass	0.63 ± 0.06	1.47 ± 0.16	1.6 ± 0.3	0.79 ± 0.13	3.3 ± 0.4	0.68 ± 0.11	0.043 ± 0.011	0.003 ± 0.003
AdoR (high Ba)	0.681 ± 0.029	1.38 ± 0.08	1.6 ± 0.3	0.52 ± 0.08	2.72 ± 0.24	0.45 ± 0.06	0.027 ± 0.006	0.0020 ± 0.0020
All other angrites (low Ba)	0.61 ± 0.03	1.51 ± 0.09	1.6 ± 0.3	0.92 ± 0.08	3.61 ± 0.26	0.78 ± 0.06	0.050 ± 0.011	0.004 ± 0.004

References

Alexander Jr., E.C., Lewis, R.S., Reynolds, J.H., Michel, M.C., 1971. Plutonium-244: Confirmation as an extinct radioactivity. *Science* **172**, 837–840.

Amelin, Y., Krot, A.N., Hutcheon, I.D., Ulyanov, A.A., 2002. Lead isotopic ages of chondrules and calcium–aluminum-rich inclusions. *Science* **297**, 1678–1683.

Baker, J., Bizzarro, M., Wittig, N., Connelly, J., Haack, H., 2005. Early planetesimal melting from an age of 4.5662 Gyr for differentiated meteorites. *Nature* **436**, 1127–1131.

Bischoff, A., Clayton, R.N., Markl, G., Mayeda, T.K., Palme, H., Schultz, L., Srinivasan, G., Weber, H.W., Weckwerth, G., Wolf, D., 2000. Mineralogy, chemistry, noble gases, and oxygen- and magnesium-isotopic compositions of the angrite Sahara 99555. *Meteorit. Planet. Sci. Suppl.* **35**, A27.

Bogard, D.D., Clayton, R.N., Marti, K., Owen, T., Turner, G., 2001. Martian volatiles: isotopic composition, origin, and evolution. *Space Sci. Rev.* **96**, 425–458.

Boynton, W.V., 1978. Fractionation in the solar nebula, II. Condensation of Th, U, Pu and Cm. *Earth Planet. Sci. Lett.* **40**, 63–70.

Burbine, T.H., McCoy, T.J., Binzel, R.P., 2001. Spectra of angrites and possible parent bodies. *Lunar Planet. Sci. XXXII*, Lunar Planet. Inst., Houston #1857 (abstr.).

Busemann, H., Baur, H., Wieler, R., 2000. Primordial noble gases in "phase Q" in carbonaceous and ordinary chondrites studied by closed-system stepped etching. *Meteorit. Planet. Sci.* **35**, 949–973.

Busemann, H., Baur, H., Wieler, R., 2003a. Solar noble gases in enstatite chondrites and implications for the formation of the terrestrial planets. *Lunar Planet. Sci. XXXIV*, Lunar Planet. Inst., Houston #1665 (abstr.).

Busemann, H., Eugster, O., Baur, H., Wieler, R., 2003b. The ingredients of the "subsolar" noble gas component. *Lunar Planet. Sci. XXXIV*, Lunar Planet. Inst., Houston #1674 (abstr.).

Busemann, H., Busfield, A., Gilmour, J.D., 2005. Ancient volcanic xenon in single glass grains from the D'Orbigny angrite. *Lunar Planet. Sci. XXXVI*, Lunar Planet. Inst., Houston #2299 (abstr.).

Busemann, H., Eugster, O., 2002. The trapped noble gas component in achondrites. *Meteorit. Planet. Sci.* **37**, 1865–1891.

Busemann, H., Eugster, O., 2003. Plutonium–xenon systematics of angrites. *Meteorit. Planet. Sci. Suppl.* **38**, A104.

Carlson, R.W., Lugmair, G.W., 2000. Timescales of planetesimal formation and differentiation based on extinct and extant radioisotopes. In: Canup, R.M., Righter, K. (Eds.), *Origin of the Earth and Moon*. The University of Arizona Press, Tucson, AZ, pp. 25–44.

Chen, J.H., Wasserburg, G.J., 1985. U–Th–Pb isotopic studies on meteorite ALHA81005 and Ibitira. *Lunar Planet. Sci.* **XVI**, 119–120.

Crabb, J., Anders, E., 1981. Noble gases in E-chondrites. *Geochim. Cosmochim. Acta* **45**, 2443–2464.

Crozaz, G., 1994. A reevaluation of the ^{244}Pu chronometer. *Mineral. Mag.* **58A**, 201–202.

Crozaz, G., Pellas, P., Bourot-Denise, M., de Chazal, S.M., Fiéni, C., Lundberg, L.L., Zinner, E., 1989. Plutonium, uranium and rare earths in the phosphates of ordinary chondrites—the quest for a chronometer. *Earth Planet. Sci. Lett.* **93**, 157–169.

Ebihara, M., Hirayama, K., Oura, Y., Miura, Y.N., Nagao, K., 2000. Chemical fractionation of rare earth elements, thorium, uranium, and plutonium in eucrites Millbillillie and Camel Donga. *Meteorit. Planet. Sci.* **35**, A50.

Eikenberg, J., Signer, P., Wieler, R., 1993. U–Xe, U–Kr, and U–Pb systematics for dating uranium minerals and investigations of the production of nucleogenic neon and argon. *Geochim. Cosmochim. Acta* **57**, 1053–1069.

Ekström, L.P., Firestone, R.B., 1999. WWW Table of radioactive isotopes, database version 2/28/99.

Eugster, O., 1988. Cosmic-ray production rates for ^{3}He, ^{21}Ne, ^{38}Ar, ^{83}Kr, and ^{126}Xe in chondrites based on ^{81}Kr–Kr exposure ages. *Geochim. Cosmochim. Acta* **52**, 1649–1662.

Eugster, O., 2003. Cosmic-ray exposure ages of meteorites and lunar rocks and their significance. *Chem. Erde* **63**, 3–30.

Eugster, O., Busemann, H., Kurat, G., Lorenzetti, S., Varela, M.E., 2002. Characterization of the noble gases and CRE age of the D'Orbigny angrite. *Meteorit. Planet. Sci. Suppl.* **37**, A44.

Eugster, O., Lorenzetti, S., 2001. Exposure history of some differentiated and lunar meteorites. *Meteorit. Planet. Sci. Suppl.* **36**, A54–A55.

Eugster, O., Michel, Th., 1995. Common asteroid break-up events of eucrites, diogenites, and howardites and cosmic-ray production rates for noble gases in achondrites. *Geochim. Cosmochim. Acta* **59**, 177–199.

Eugster, O., Michel, Th., Niedermann, S., 1991. ^{244}Pu–Xe formation and gas retention age, exposure history, and terrestrial age of angrites LEW86010 and LEW87051: comparison with Angra dos Reis. *Geochim. Cosmochim. Acta* **55**, 2957–2964.

Eugster, O., Michel, Th., Niedermann, S., Wang, D., Yi, W., 1993. The record of cosmogenic, radiogenic, fissiogenic, and trapped noble gases in recently recovered Chinese and other chondrites. *Geochim. Cosmochim. Acta* **57**, 1115–1142.

Feigelson, E.D., Montmerle, T., 1999. High-energy processes in young stellar objects. *Annu. Rev. Astron. Astrophys.* **37**, 363–408.

Fleming, W.H., Thode, H.G., 1953. Neutron and spontaneous fission in uranium ores. *Phys. Rev.* **92**, 378–382.

Floss, C., Crozaz, G., McKay, G., Mikouchi, T., Killgore, M., 2003. Petrogenesis of angrites. *Geochim. Cosmochim. Acta* **67**, 4775–4789.

Flynn, K.F., Srinivasan, B., Manuel, O.K., Glendenin, L.E., 1972. Distribution of mass and charge in the spontaneous fission of ^{244}Cm. *Phys. Rev. C* **6**, 2211–2214.

Ganapathy, R., Anders, E., 1969. Ages of calcium-rich achondrites: II. Howardites, nakhlites, and the Angra dos Reis angrite. *Geochim. Cosmochim. Acta* **33**, 775–787.

Garrison, D., Bogard, D., 2003. ^{39}Ar–^{40}Ar age dating of two angrites and two brachinites. *Lunar Planet. Sci. XXXIV*, Lunar Planet. Inst., Houston #1069 (abstr.).

Garrison, D.H., Bogard, D.D., Lindstrom D.J., 1998. An unusual melt glass with fission Xe in eucrite EET90020: evidence for a primitive phase enriched in U, ^{244}Pu, and LREE. *Lunar Planet. Sci. XXIX*, Lunar Planet. Inst., Houston #1297 (abstr.).

Geiss, J., Bühler, F., Cerutti, H., Eberhardt, P., Filleux, C., 1972. Solar wind composition experiment. *Apollo 16 Prelim. Sci. Rep. NASA SP-315*, 14.1–14.10.

Glavin, D.P., Kubny, A., Jagoutz, E., Lugmair, G.W., 2004. Mn–Cr isotope systematics of the D'Orbigny angrite. *Meteorit. Planet. Sci.* **39**, 693–700.

Graham, D.W., 2002. Noble gas isotope geochemistry of mid-ocean ridge and ocean island basalts: characterization of mantle source reservoirs. *Rev. Mineral. Geochem.* **47**, 247–317.

Greenwood, R.C., Franchi, I.A., Jambon, A., 2003. Oxygen isotope evidence for the origin of HEDs and angrites. *Meteorit. Planet. Sci.* **38**, A96.

Greenwood, R.C., Franchi, I.A., Jambon, A., Buchanan, P.C., 2005. Widespread magma oceans on asteroidal bodies in the early Solar System. *Nature* **435**, 916–918.

Grimberg, A., Bühler, F., Burnett, D.S., Jurewicz, A.J.G., Hays, C.C., Bochsler, P., Heber, V.S., Baur, H., Wieler, R., 2006. Solar wind helium and neon from metallic glass flown on Genesis—preliminary bulk and velocity-dependent data. *Lunar Planet. Sci. XXXVII*, Lunar Planet. Inst., Houston #1782 (abstr.).

Hebeda, E.H., Schultz, L., Freundel, M., 1987. Radiogenic, fissiogenic and nucleogenic noble gases in zircons. *Earth Planet. Sci. Lett.* **85**, 79–90.

Hohenberg, C.M., 1970. Xenon from the Angra dos Reis meteorite. *Geochim. Cosmochim. Acta* **34**, 185–191.

Hohenberg, C.M., Bernatowicz, T.J., Podosek, F.A., 1991. Comparative xenonology of two angrites. *Earth Planet. Sci. Lett.* **102**, 167–177.

Hohenberg, C.M., Hudson, B., Kennedy, B.M., Podosek, F.A., 1981. Xenon spallation systematics in Angra dos Reis. *Geochim. Cosmochim. Acta* **45**, 1909–1915.

Hudson, B., Hohenberg, C.M., Kennedy, B.M., Podosek, F.A., 1982. ^{244}Pu in the early solar system. *Lunar Planet. Sci.* **XIII**, 346–347.

Hyde, E.K., Perlman, I., Seaborg, G.T., 1964. *The Nuclear Properties of the Heavy Elements*. Prentice-Hall, Englewood Cliffs, NJ.

Jacobsen, S.B., Wasserburg, G.J., 1984. Sm–Nd isotopic evolution of chondrites and achondrites, II. *Earth Planet. Sci. Lett.* **67**, 137–150.

Jagoutz, E., Jotter, R., Kubny, A., Varela, M.E., Zartman, R., Kurat, G., Lugmair, G.W., 2003. Cm?-U–Th–Pb isotopic evolution of the D'Orbigny angrite. *Meteorit. Planet. Sci. Suppl.* **38**, A81.

Jagoutz, E., Jotter, R., Varela, M.E., Zartman, R., Kurat, G., Lugmair, G.W., 2002. Pb–U–Th isotopic evolution of the D'Orbigny angrite. *Lunar Planet. Sci. XXXIII*, Lunar Planet. Inst., Houston #1043 (abstr.).

Jambon, A., Barrat, J.A., Boudouma, O., Fonteilles, M., Badia, D., Göpel, C., Bohn, M., 2005. Mineralogy and petrology of the angrite Northwest Africa 1296. *Meteorit. Planet. Sci.* **40**, 361–375.

Jones, J.H., 1982. The geochemical coherence of Pu and Nd and the ^{244}Pu/^{238}U ratio of the early solar system. *Geochim. Cosmochim. Acta* **46**, 1793–1804.

Jotter, R., Jagoutz, E., Varela, M.E., Zartman, R., Kurat, G., 2003. Lead isotopic study of glasses from the D'Orbigny angrite. *Meteorit. Planet. Sci. Suppl.* **38**, A53.

Jurewicz, A.J.G., Jones, J.H., Mittlefehldt, D.W., Longhi, J., 2004. Devolatilized-Allende partial melts as an analog for primitive angrite magmas. *Lunar Planet. Sci. XXXV*, Lunar Planet. Inst., Houston #1417 (abstr.).

Jurewicz, A.J.G., Mittlefehldt, D.W., Jones, J.H., 1993. Experimental partial melting of the Allende (CV) and Murchison (CM) chondrites and the origin of asteroidal basalts. *Geochim. Cosmochim. Acta* **57**, 2123–2139.

Kuehner, S.M., Irving, A.J., Bunch, T.E., Wittke, J.H., Hupé, G.M., 2006. Coronas and symplectities in plutonic angrite NWA 2999 and implications for Mercury as the angrite parent body. *Lunar Planet. Sci. XXXVII*, Lunar Planet. Inst., Houston #1344 (abstr.).

Kurat, G., Brandstätter, F., Clayton, R., Nazarov, M.A., Palme, H., Schultz, L., Varela, M.E., Wäsch, E., Weber, H.W., Weckwerth, G., 2001. D'Orbigny: a new and unusual angrite. *Lunar Planet. Sci. XXXII*, Lunar Planet. Inst., Houston #1753 (abstr.).

Kurat, G., Varela, M.E., Brandstätter, F., Weckwerth, G., Clayton, R.N., Weber, H.W., Schultz, L., Wäsch, E., Nazarov, M.A., 2004. D'Orbigny: A non-igneous angritic achondrite? *Geochim. Cosmochim. Acta* **68**, 1901–1921.

Lavielle, B., Marti, K., Pellas, P., Perron, C., 1992. Search for ^{248}Cm in the early solar system. *Meteoritics* **27**, 382–386.

Leich, D.A., Niemeyer, S., Michel, M.C., 1977. Elimination of ^{248}Cm as a possible progenitor of carbonaceous chondrite fission xenon. *Earth Planet. Sci. Lett.* **34**, 197–208.

Lewis, R.S., 1975. Rare gases in separated whitlockite from the St. Severin chondrite: xenon and krypton from fission of extinct ^{244}Pu. *Geochim. Cosmochim. Acta* **39**, 417–432.

Leya, I., Lange, H.-J., Neumann, S., Wieler, R., Michel, R., 2000. The production of cosmogenic nuclides in stony meteoroids by galactic cosmic-ray particles. *Meteorit. Planet. Sci.* **35**, 259–286.

Lugmair, G.W., Galer, S.J.G., 1992. Age and isotopic relationships among the angrites Lewis Cliff 86010 and Angra dos Reis. *Geochim. Cosmochim. Acta* **56**, 1673–1694.

Lugmair, G.W., Marti, K., 1977. Sm–Nd–Pu timepieces in the Angra dos Reis meteorite. *Earth Planet. Sci. Lett.* **35**, 273–284.

Lugmair, G.W., Shukolyokov, A., 1998. Early solar system timescales according to ^{53}Mn–^{53}Cr systematics. *Geochim. Cosmochim. Acta* **62**, 2863–2886.

Ma, M.-S., Murali, A.V., Schmitt, R.A., 1977. Genesis of the Angra dos Reis and other achondritic meteorites. *Earth Planet. Sci. Lett.* **35**, 331–346.

MacNamara, J., Thode, H.G., 1950. The isotopes of xenon and krypton in pitchblende and the spontaneous fission of U^{238}. *Phys. Rev.* **80**, 471–472.

Manhès, G., Göpel, C., Allègre, C.J., 1987. High resolution chronology of the early solar system based on lead isotopes. *Meteoritics* **22**, 453–454.

Marti, K., Eberhardt, P., Geiss, J., 1966. Spallation, fission, and neutron capture anomalies in meteoritic krypton and xenon. *Z. Naturforsch.* **21a**, 398–413.

Marti, K., Kim, J.S., Lavielle, B., Pellas, P., Perron, C., 1989. Xenon in chondritic metal. *Z. Naturforsch.* **44a**, 963–967.

Marty, B., Lussiez, P., 1993. Constraints on rare gas partition coefficients from analysis of olivine–glass from a picritic mid-ocean ridge basalt. *Chem. Geol.* **106**, 1–7.

Mason, B., Graham, A.L., 1970. Minor and trace elements in meteoritic minerals. *Smithson. Contrib. Earth Sci.* **3**, 1–17.

McCoy, T.J., Ketcham, R.A., Benedix, G.K., Carlson, W.D., Wilson, L., 2002. Vesicular basalts from asteroids: clues to physical processes in their parent magmas. *Lunar Planet. Sci. XXXIII*, Lunar Planet. Inst., Houston #1213 (abstr.).

McCoy, T.J., Wilson, L., Benedix, G.K., Ketcham, R.A., 2003. Vesicles in meteorites: the angle on angrites. *Meteorit. Planet. Sci. Suppl.* **38**, A65.

McKay, G., Ogawa, T., Miyamoto, M., Takeda, H., 1993. More on the cooling history of angrite LEW 86010. *Lunar Planet. Sci.* **XXIV**, 967–968.

Mikouchi, T., McKay, G., 2001. Mineralogical investigation of D'Orbigny: a new angrite showing close affinities to Asuka 881371, Sahara 99555 and Lewis Cliff 87051. *Lunar Planet. Sci. XXXII*, Lunar Planet. Inst., Houston #1876 (abstr.).

Mikouchi, T., McKay, G., Koizumi, E., Monkawa, A., Miyamoto, M., 2003. Northwest Africa 1670: a new quenched angrite. *Meteorit. Planet. Sci.* **38**, A115.

Mikouchi, T., McKay, G., Le, L., Mittlefehldt, D.W., 2000. Preliminary examination of Sahara 99555: mineralogy and experimental studies of a new angrite. *Lunar Planet. Sci. XXXI*, Lunar Planet. Inst., Houston #1970 (abstr.).

Mikouchi, T., Miyamoto, M., McKay, G.A., 1996. Mineralogical study of angrite Asuka-881371: its possible relation to angrite LEW87051. *Proc. NIPR Symp. Antarct. Met.* **9**, 174–188.

Mittlefehldt, D.W., Killgore, M., Lee, M.T., 2002. Petrology and geochemistry of D'Orbigny, geochemistry of Sahara 99555, and the origin of angrites. *Meteorit. Planet. Sci.* **37**, 345–369.

Mittlefehldt, D.W., Lindstrom, M.M., 1990. Geochemistry and genesis of the angrites. *Geochim. Cosmochim. Acta* **54**, 3209–3218.

Miura, Y.N., Sugiura, N., Kusakabe, M., Nagao, K., 2004. Noble gases in Northwest Africa 1670, a new angrite, and oxygen isotopes of this angrite and some achondrites. *Antarct. Met. XXVIII*, 50–51.

Mizote, S., Matsumoto, T., Matsuda, J.-I., Koeberl, C., 2003. Noble gases in Muong Nong-type tektites and their implications. *Meteorit. Planet. Sci.* **38**, 747–758.

Mizuno, H., Nakazawa, K., Hayashi, C., 1980. Dissolution of the primordial rare gases into the molten earth's material. *Earth Planet. Sci. Lett.* **50**, 202–210.

Müller, H.W., Zähringer, J., 1969. Rare gases in stony meteorites. In: Millman, P.M. (Ed.), *Meteorite Research*. D. Reidel Publishing Co, Dordrecht, pp. 845–856.

Munk, M.N., 1967. Argon, krypton, and xenon in Angra dos Reis, Nuevo Laredo, and Norton County achondrites: the case for two types of fission Xe in achondrites. *Earth Planet. Sci. Lett.* **3**, 457–465.

Nuccio, P.M., Paonita, A., 2000. Investigation of the noble gas solubility in H_2O–CO_2 bearing silicate liquids at moderate pressure II: the extended ionic porosity (EIP) model. *Earth Planet. Sci. Lett.* **183**, 499–512.

Nyquist, L., Bogard, D.D., 2003. Isotopic studies of basaltic meteorites: constraints on the size and thermal history of differentiated asteroids. In: *NIPR Symposium on Evolution Solar System Materials*.

Nyquist, L.E., Bansal, B., Wiesmann, H., Shih, C.-Y., 1994. Neodymium, strontium and chromium isotopic studies of the LEW86010 and Angra dos Reis meteorites and the chronology of the angrite parent body. *Meteoritics* **29**, 872–885.

Nyquist, L.E., Shih, C.Y., Wiesmann, H., Mikouchi, T., 2003. Fossil ^{26}Al and ^{53}Mn in D'Orbigny and Sahara 99555 and the timescale for angrite magmatism. *Lunar Planet. Sci. XXXIV*, Lunar Planet. Inst., Houston #1388 (abstr.).

Okazaki, R., Takaoka, N., Nagao, K., Sekiya, M., Nakamura, T., 2001. Noble-gas-rich chondrules in an enstatite meteorite. *Nature* **412**, 795–798.

Papike, J.J., Karner, J.M., Shearer, C.K., 2003. Determination of planetary basalt parentage: a simple technique using the electron microprobe. *Am. Mineral.* **88**, 469–472.

Pepin, R.O., 1991. On the origin and early evolution of terrestrial planet atmospheres and meteoritic volatiles. *Icarus* **92**, 2–79.

Pfennig, G., Klewe-Nebenius, H., Seelmann-Eggebert, W., 1998. *Chart of the nuclides*, sixth ed. 1995, revised reprint. Forschungszentrum Karlsruhe GmbH.

Pinti, D.L., Matsumoto, T., Matsuda, J.-I., Fang, Z., 2004. Distribution of noble gases in Chinese tektites: implication for neon solubility in natural glasses. *Meteorit. Planet. Sci.* **39**, 87–96.

Podosek, F.A., Cassen, P., 1994. Theoretical, observational, and isotopic estimates of the lifetime of the solar nebula. *Meteoritics* **29**, 6–25.

Podosek, F.A., Woolum, D.S., Cassen, P., Nichols Jr., R.H., 2000. Solar gases in the Earth by solar wind irradiation. *J. Conf. Abstr.* **5** (2), 804.

Porcelli, D., Woolum, D., Cassen, P., 2001. Deep Earth rare gases: initial inventories, capture from the solar nebula, and losses during Moon formation. *Earth Planet. Sci. Lett.* **193**, 237–251.

Premo, W.R., Tatsumoto, M., 1995. Pb isotopic systematics of angrite Asuka-881371. *Antarct. Met.* **XX**, 204–206.

Prinz, M., Weisberg, M.K., 1995. Asuka 881371 and the angrites: origin in a heterogeneous, CAI-enriched, differentiated, volatile-depleted body. *Antarct. Met.* **XX**, 207–210.

Prinzhofer, A., Papanastassiou, D.A., Wasserburg, G.J., 1992. Samarium–neodymium evolution of meteorites. *Geochim. Cosmochim. Acta* **56**, 797–815.

Quitté, G., Birck, J.-L., Allègre, C.J., 2000. ^{182}Hf-^{182}W systematics in eucrites: the puzzle of iron segregation in the early solar system. *Earth Planet. Sci. Lett.* **184**, 83–94.

Rao, M.N., Gopalan, K., 1973. Curium-248 in the early solar system. *Nature* **245**, 304–307.

Sasaki, S., 1991. Off-disk penetration of ancient solar wind. *Icarus* **91**, 29–38.

Schnetzler, C.C., Philpotts, J.A., 1969. Genesis of the calcium-rich achondrites in light of rare-earth and barium concentrations. In: Millman, P.M. (Ed.), *Meteorite Research*. D. Reidel Publishing Co, Dordrecht, pp. 206–216.

Shukolyukov, A., Begemann, F., 1996. Pu–Xe dating of eucrites. *Geochim. Cosmochim. Acta* **60**, 2453–2471.

Spivak-Birndorf, L., Wadhwa, M., Janney, P.E., 2005. ^{26}Al–^{26}Mg chronology of the D'Orbigny and Sahara 99555 angrites. *Meteorit. Planet. Sci. Suppl.* **40**, A145.

Srinivasan, B., Alexander Jr., E.C., Manuel, O.K., Troutner, D.E., 1969. Xenon and krypton from the spontaneous fission of californium-252. *Phys. Rev.* **179**, 1166–1169.

Srinivasan, B., Flynn, K.F., 1980. Kr and Xe isotopes from spontaneous fission of ^{248}Cm and ^{250}Cf: comparison with noble gases in carbonaceous chondrites. *Earth Planet. Sci. Lett.* **47**, 235–242.

Stirling, C.H., Halliday, A.N., Porcelli, D., 2005. In search of live ^{247}Cm in the early solar system. *Geochim. Cosmochim. Acta* **69**, 1059–1071.

Störzer, D., Pellas, P., 1977. Angra dos Reis: plutonium distribution and cooling history. *Earth Planet. Sci. Lett.* **35**, 285–293.

Sugiura, N., 2002. Mn–Cr chronology of olivine in some meteorites. *Lunar Planet. Sci. XXXIII*, Lunar Planet. Inst., Houston #1435 (abstr.).

Sugiura, N., Hashizume, K., Miyazaki, A., Yanai, K., 2003. Mn–Cr ages of two angrites. In: *NIPR Symposium on Evolution Solar System Materials*.

Swindle, T.D., Garrison, D.H., Goswami, J.N., Hohenberg, C.M., Nichols, R.H., Olinger, C.T., 1990. Noble gases in the howardites Bholghati and Kapoeta. *Geochim. Cosmochim. Acta* **54**, 2183–2194.

Tatsumoto, M., Knight, R.J., Allegre, C.J., 1973. Time differences in the formation of meteorites as determined from the ratio of lead-207 to lead-206. *Science* **180**, 1279–1283.

Taylor, G.J., Keil, K., McCoy, T., Haack, H., Scott, E.R.D., 1993. Asteroid differentiation: pyroclastic volcanism to magma oceans. *Meteoritics* **28**, 34–52.

Tera, F., Eugster, O., Burnett, D.S., Wasserburg, G.J., 1970. Comparative study of Li, Na, K, Rb, Cs, Ca, Sr and Ba abundances in achondrites and in Apollo 11 lunar samples. In: *Proceedings of the Apollo 11 Lunar Science Conference*, pp. 1637–1657.

Tolstikhin, I., Hofmann, A.W., 2005. Early crust on top of the Earth's core. *Phys. Earth Planet. Inter.* **148**, 109–130.

Tonui, E.K., Ngo, H.H., Papanastassiou, D.A., 2003. Rb–Sr and Sm–Nd study of the D'Orbigny angrite. *Lunar Planet. Sci. XXXIV*, Lunar Planet. Inst., Houston #1812 (abstr.).

Varela, M.E., Kurat, G., Zinner, E., Hoppe, P., Ntaflos, T., Nazarov, M.A., 2005. The non-igneous genesis of angrites: support from trace element distribution between phases in D'Orbigny. *Meteorit. Planet. Sci.* **40**, 409–430.

Varela, M.E., Kurat, G., Zinner, E., Métrich, N., Brandstätter, F., Ntaflos, T., Sylvester, P., 2003. Glasses in the D'Orbigny angrite. *Geochim. Cosmochim. Acta* **67**, 5027–5046.

Wadhwa, M., Russell, S.S., 2000. Timescales of accretion and differentiation in the early solar system: the meteoritic evidence. In: Mannings, V., Boss, A.P., Russell, S.S. (Eds.), *Protostars and Planets IV*. University of Arizona Press, Tucson, AZ, pp. 995–1018.

Warren, P.H., Davis, A.M., 1995. Consortium investigation of the Asuka-881371 angrite: petrographic, electron microprobe, and ion microprobe observations. *Antarct. Met.* **XX**, 257–260.

Wasserburg, G.J., Tera, F., Papanastassiou, D.A., Huneke, J.C., 1977. Isotopic and chemical investigations on Angra dos Reis. *Earth Planet. Sci. Lett.* **35**, 294–316.

Weigel, A., Eugster, O., Koeberl, C., Krähenbühl, U., 1997. Differentiated achondrites Asuka 881371, an angrite, and Divnoe: noble gases, ages, chemical composition, and relation to other meteorites. *Geochim. Cosmochim. Acta* **61**, 239–248.

Wetherill, G.W., 1953. Spontaneous fission yields from Uranium and Thorium. *Phys. Rev.* **92**, 907–912.

Wieler, R., 1998. The solar noble gas record in lunar samples and meteorites. *Space Sci. Rev.* **85**, 303–314.

Wieler, R., 2002a. Cosmic-ray-produced noble gases in meteorites. *Rev. Mineral. Geochem.* **47**, 125–170.

Wieler, R., 2002b. Noble gases in the solar system. *Rev. Mineral. Geochem.* **47**, 21–70.

Wieler, R., Busemann, H., Franchi, I.A., 2006. Trapping and modification processes of noble gases and nitrogen in meteorites and their parent bodies. In: Lauretta, D.S., Leshin, L.A., McSween, H.Y. (Eds.), *Meteorites and the Early Solar System II*. University of Arizona Press, Tucson, AZ, pp. 499–521.

Wilson, L., Keil, K., 1991. Consequences of explosive eruptions on small solar system bodies: the case of the missing basalts on the aubrite parent body. *Earth Planet. Sci. Lett.* **104**, 505–512.

Woolum, D.S., Burnett, D.S., 1975. In-situ measurement of the rate of ^{235}U fission induced by lunar neutrons. *Earth Planet. Sci. Lett.* **21**, 153–163.